“Design and synthesis of triazatruxene based donor acceptor molecules”

M.Sc. Thesis

by

Prashant Kumar

DEPARTMENT OF CHEMISTRY
INDIAN INSTITUTE OF TECHNOLOGY
INDORE

May 2026

"Design and synthesis of triazatruxene based donor acceptor molecules"

A THESIS

Submitted in partial fulfilment of the
requirements for the award of the degree
of

Master of Science

by

Prashant Kumar

DEPARTMENT OF CHEMISTRY
INDIAN INSTITUTE OF TECHNOLOGY
INDORE

May 2026

INDIAN INSTITUTE OF TECHNOLOGY
INDORE
CANDIDATE'S DECLARATION

I hereby certify that the work which is being presented in this thesis entitled report entitled "**Design and synthesis triazatruxene based donor-acceptor molecule**" where I have done "**Design and Synthesis of Different Donor-Acceptor Based molecules**", in the partial fulfilment of the requirements for the award of the degree of **MASTER OF SCIENCE** and submitted to the **DEPARTMENT OF CHEMISTRY, Indian Institute of Technology Indore,** is an authentic record of my own work carried out during the time period from July 2025 to May 2026 of M.Sc. project work under the supervision of Prof. Rajneesh Misra, IIT Indore.

The matter presented in this thesis has not been submitted by me for the award of any other degree of this or any other institute.

Prashant Kumar 21/05/26

Signature of the student with date
(Prashant Kumar)

This is to certify that the above statement made by the candidate is correct to the best of my knowledge.



Signature of the Supervisor of M.Sc. thesis
(Prof. Rajneesh Misra)

Prashant Kumar has successfully given the oral his M.Sc. The oral Examination held on 21 **May 2026**

ACKNOWLEDGEMENT

With great pleasure, I would like to express my deep sense of gratitude to my supervisor **Prof. Rajneesh Misra**, for giving me a wonderful opportunity to pursue research and for believing in my research abilities. His constant guidance, support and motivation have been immensely helpful to complete this M.Sc. project. His enthusiasm and dedication have always inspired me. Further, I would like to thank my PSPC members **Prof. Rajneesh Misra** and **Prof. Sampak Samanta** for their valuable suggestions and support.

I wish to express my gratitude to Prof. Suhas S. Joshi, Director, IIT Indore for his continuous encouragement, help, and support in every aspect. I am grateful to Dr. Umesh Kshirsagar (Head, Department of Chemistry, IIT Indore). I am also grateful to Prof. Suman Mukhopadhyay, Prof. Sanjay Singh, Prof. Apurba Kumar Das, Dr. Shaikh M. Mobin, Dr. Anjan Chakraborty, Dr. Satya S. Bulusu, Prof. Biswarup Pathak, Prof. Sampak Samanta, Dr. Tridib Kumar Sarma, and Dr. Chelvam Venkatesh, Dr. Selvakumar Sermadurai, Dr. Abhinav Raghuvanshi, Dr. Amrendra Kumar Singh and Dr. Tushar K. Mukherjee, for the help during various activities. I would like to extend my sincere thanks to my mentor Kusum Yadav for their supportive, kind and friendly nature. I extend my deep thanks to my group members Dr. Mohd. Wazid, Nikhil Ji Tiwari, Ramakant Gavale, Amiy Krishna, Nitin Rajesh, Shivangi, Akansha, Vivek, Kushagra, Anurag, Dhuruv and Harshal for their selfless co-operation and help to make my work successful. I would also like to thank the technical staff from Sophisticated Instrumentation Centre (SIC), IIT Indore, Mr. Kinny Pandey, Mr. Ghanshyam Bhavsar for their patience and timely technical support without which it was impossible to continue with my work. I personally want to extend my thanks to my batch mates Mahesh, Akshay, Rahul, Vishal and Sounak who were always there and never let me down during these M.Sc. days.

Here, it is to be specially mentioned that, none of this would have been possible without the support of my family and I deeply express my love and gratitude to my parents.

Prashant Kumar

DEDICATION

Every challenging work needs self-endeavour and the blessings of elders.

My modest effort I dedicate to my concern and supporting

FAMILY

Whose motivation, love, and encouragement

make me able to complete my work efficiently.

Along with all inspiring and respected

TEACHERS

ABSTRACT

Triazatruxene (TAT) stands out as a highly researched aromatic compound, thanks to its distinctive optical and electronic characteristics, affordability, and ease of modification. Recently, TAT and its derivatives have emerged as a versatile foundation for creating materials with a broad spectrum of uses. Its electron–rich nitrogen atoms enhance its electron donation capabilities and its planar structure helps to improve the charge carrier mobility in electronic devices. This work involves the synthesis and characterization of triazatruxene–based derivatives: **TAT1** and **TAT2**, obtained *via* reaction of intermediate **5** with tetracyanoethylene (TCNE) and 7,7,8,8-tetracyanoquinodimethane (TCNQ) respectively, generating tetracyanobutadiene (TCBD)–functionalized **TAT1** and dicyanomethylene-expanded–TCBD (DCNQ)–functionalized **TAT2**. The photophysical, electrochemical and theoretical studies were explored which shows good donor–acceptor interaction and successful tuning of the HOMO-LUMO band gap.

TABLE OF CONTENTS

	LIST OF FIGURES……...	13
	LIST OF SCHEMES……	14
	ABBREVIATIONS……...	15
	ACRONYMS……	16
Chapter 1.	**Introduction……...**	17-22
1.1	General Introduction……	17-21
1.2	Aim and Strategy of our work…….	21-22
Chapter 2.	**Literature Review……..**	23-26
Chapter 3.	**Experimental Section……**	27-31
3.1	Chemicals, reagent and methods…….	27
3.2	Experimental Procedure……	27
3.2.1	Synthesis and characterization of Compound **1**……...	27
3.2.2	Synthesis and characterization of Compound **2**……...	28
3.2.3	Synthesis and characterization of Compound **3**……...	28
3.2.4	Synthesis and characterization of Compound **4**……...	28
3.2.5	Synthesis and characterization of Compound **5**……..	29
3.2.6	Synthesis and characterization of Compound **TAT1...**	30
3.2.7	Synthesis and characterization of Compound **TAT2**...	30-31
Chapter 4.	**Result and Discussion……**	32-38
	Conclusion and scope of our work……..	39
	APPENDIX-A NMR, HRMS……	40-48
	REFERENCES……...	49-53

LIST OF FIGURES AND TABLES

Figure 1.1. Schematic presentation of charge-transfer in triazatruxene based in a push-pull systems.

Figure 1.2. Different type of donors.

Figure 1.3. Different type of acceptors.

Figure 1.4. Structure of triazatruxene.

Figure 1.5. The molecular structures of **TCNE** and **TCNQ**.

Figure 1.6. Chemical structure of **TAT1** and **TAT2.**

Figure 2. Normalized absorption spectra of **TAT1** and **TAT2.**

Figure 3. CVs plots of **TAT1**and **TAT2**.

Figure 4. The FMOs of **TAT1** and **TAT2** at the B3LYP/6-311+G (d,p) level.

Figure 5. ^{1}H NMR spectrum of compound **1**.

Figure 6. ^{13}C NMR spectrum of compound **1**.

Figure 7. HRMS of compound **1**.

Figure 8. ^{1}H NMR spectrum of compound **2**.

Figure 9. ^{13}C NMR spectrum of compound **2**.

Figure 10. HRMS of compound **2**.

Figure 11. ^{1}H NMR spectrum of **4**.

Figure 12. ^{13}C NMR spectrum of **4.**

Figure 13. HRMS of compound **4.**

Figure 14. ^{1}H NMR of compound **5.**

Figure 15. ^{13}C NMR of compound **5.**

Figure 16. HRMS of compound **5.**

Figure 17. ^{1}H NMR of **TAT1.**

Figure 18. ^{13}C NMR of **TAT1.**

Figure 19. HRMS of **TAT1**.

Figure 20. ^{1}H NMR spectrum of **TAT2**.

Figure 21. ^{13}C NMR spectrum of **TAT2**.

Figure 22. HRMS of **TAT2**.

Table 1. Photophysical and theoretical data of **TAT1** and **TAT2.**

Table 2. Electrochemical data of **TAT1** and **TAT2.**

LIST OF SCHEMES

Scheme 1. Synthetic pathway to intermediate **1-5.**

Scheme 2.1 Synthetic pathway by Bergman *et al.*

Scheme 2.2 Synthetic pathway of triazatruxene and tetraindole synthesis.

Scheme 2.3 Michael method for TCNE derivative synthesis.

Scheme 2.4 Yoshiro method for TCNE derivative synthesis.

Scheme 2.5 Francois Diederich method for TCNE derivative synthesis

Scheme 4.1. Synthetic pathway for Compound **1.**

Scheme 4.2. Synthetic pathway for Compound **2.**

Scheme 4.3. Synthetic pathway for Compound **3.**

Scheme 4.4. Synthetic pathway for Compound **4.**

Scheme 4.5. Synthetic pathway for Compound **5.**

Scheme 4.6. Synthetic pathway for Compound **TAT1.**

Scheme 4.7. Synthetic pathway for Compound **TAT2.**

ABBREVIATIONS

mg	Milligram
mol	Mole
g	Gram
℃	Degree Celsius
%	Percentage
h	Hours
min	Minutes
mL	Milliliter
π	Pi
λ	Wavelength
δ	Chemical shift
eV	Electron volt
V	Volt
TAT	triazatruxene

ACRONYMS

Abbreviations used here for substituents, reagents, etc. are largely in accordance with the recommendation of the IUPAC-IUC Commission on Biochemical Nomenclature, 1974, Pure and Applied Chemistry, 40, 315-331. Additional abbreviations used in this report are listed below:

DMSO	Dimethyl sulfoxide
DMF	Dimethylformamide
PCE	Power conversion efficiency
HTM	Hole transporting materials
PSC	Perovskite solar cell
D-A-D	Donor-acceptor-donor
TPA	Triphenylamine
DCM	Dichloromethane
DFT	Density functional theory
HRMS	High-resolution mass spectrometry
NMR	Nuclear magnetic resonance
TAT	Triazatruxene
TMS	Tetramethylsilane
CT	Charge Transfer
CS	Charge Separation

Chapter-1

INTRODUCTION

The development of π–conjugated push–pull chromophores have emerged as an important class of material in recent years because of their notable optoelectronic properties. Owing to their unique properties, they have found widespread applications in various devices such as organic solar cells (OSCs)[1], organic light emitting diodes (OLEDs)[2,3], Perovskite solar cells (PSCs)[4,5] and organic field-effect transistors (OFETs). Furthermore, these chromophores are also used in sensors, security inks, fluorescent probes[6], electrochromic devices[7,8],pressure sensors, and data storage devices[9].

In donor–acceptor (D–A) systems, the donor part supplies electrons and helps in hole transport, while the acceptor part attracts electrons and supports electron transport. When these two are connected in one molecule, electrons move from the donor to the acceptor. During this transfer, electrons are promoted from the highest occupied molecular orbital (HOMO) to the lowest unoccupied molecular orbital (LUMO), creating charge separation. This process gives rise to a characteristic charge-transfer absorption band in the UV–visible region. The intensity and efficiency of this charge-transfer absorption can be enhanced by introducing π-spacers or π-linkers between the donor and acceptor units. These spacers improve conjugation and facilitate better electron movement across the molecule.

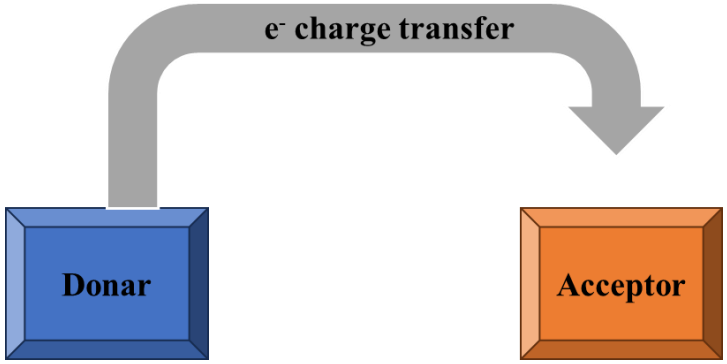


Figure 1.1. Schematic presentation of charge-transfer in triazatruxene based in a push-pull systems.

Tuning the charge-transfer band in donor–acceptor systems is very important for material science applications, especially in devices like OSCs and organic field-effect OFETs. Some well-known π-donors are triazatruxene, carbazole, phenothiazine; and acceptor groups usually contain electron-withdrawing imine units (–C=N–). Common examples include Dimethylbithiazole, dimethyltetrazine, dimethylbenzothiadiazole pyridylthiadiazole (PT)[10], bisthiazole (BTz)[11], benzobisthiazole (BBTz)[12], benzotriazole (BTA), and isoindigo[13].

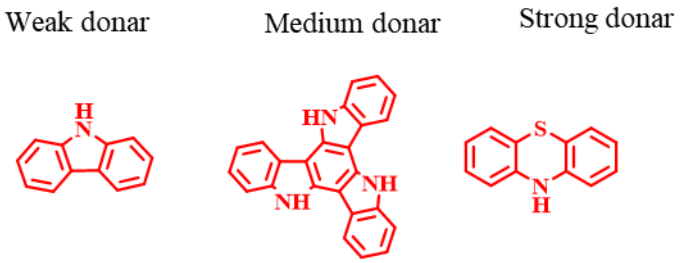


Figure 1.2. Different type of donors.

These acceptor units are generally classified as weak, medium, or strong depending on their electron-withdrawing strength. This strength is mainly determined by their LUMO energy level—units with lower LUMO energy are stronger electron acceptors.

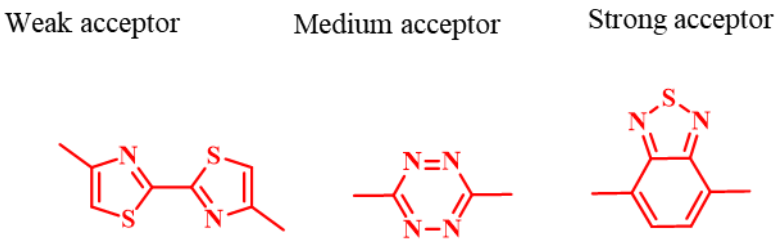
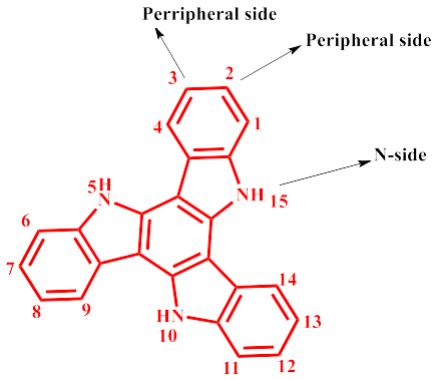


Figure 1.3. Different type of acceptors.

Triazatruxene (TAT) is an excellent donor possessing strong π–π intermolecular interaction, high hole mobility, excellent thermal stability and various functionalization sites for tuning optoelectronic properties of materials.[14,15] It has a planar structure having C3



symmetry.[16] It is very reactive towards electrophilic substitution due to three fused carbazole rings. The most

Figure 1.4 Structure of triazatruxene.

reactive positions are located on 2, 7, and 12 position. Also, in the presence of excess electrophile, the substitution may proceed further at 3, 8 and 13 positions.[17] Numerous works has been reported on hexasubstituted and trisubstituted triazatruxenes D–A based systems.[18] Recently, researchers are focusing on the monosubstituted TAT derivatives for optoelectronic applications.

Tetracyanoethylene (TCNE) and tetracyanoquinodimethane (TCNQ) are well-known strong electron acceptors. Their high electron-withdrawing ability comes mainly from the presence of cyano (–C≡N) groups, which are highly electronegative and strongly pull electron density through π-conjugation. Structurally, TCNE has a simple ethylene (C=C) core with four cyano groups attached directly to the double bond, whereas TCNQ has a larger quinodimethane framework with four cyano groups attached at the para positions.[19,20] Because of these features, both molecules can efficiently attract electrons from electron-rich systems. When TCNE or TCNQ reacts with electron-rich alkynes, they undergo a [2+2] cycloaddition reaction to form cyclobutene intermediates. These intermediates are not stable and quickly open through a retroelectrocyclization step to give highly

conjugated products such as tetracyanobutadiene (TCBD) and dicyanoquinodimethane (DCNQ) derivatives. These reactions are widely used to construct donor–acceptor (D–A) systems. D–A systems containing strong acceptors like TCBD and DCNQ are very important in organic electronics, especially in photovoltaic applications.[21,22] These molecules often show intense and broad absorption over a wide range of electromagnetic spectrum due to efficient intramolecular charge transfer.[23] They also allow precise control over the LUMO energy levels, which is crucial for device performance. The properties can be further adjusted by modifying the donor units, acceptor units, or spacer groups within the molecule. Because of these tunable features, such donor–acceptor systems are widely used in many advanced technologies, including TCBD-sensitized solar cells (DSSCs), nonlinear optical (NLO) materials, OFETs, OLEDs, bulk heterojunction solar cells, as well as in sensing, bioimaging, photodynamic therapy, and molecular switching devices.



Tetracyanoquinodimethane Tetracyanoethylene

Figure 1.5. The molecular structure of TCNE and TCNQ.

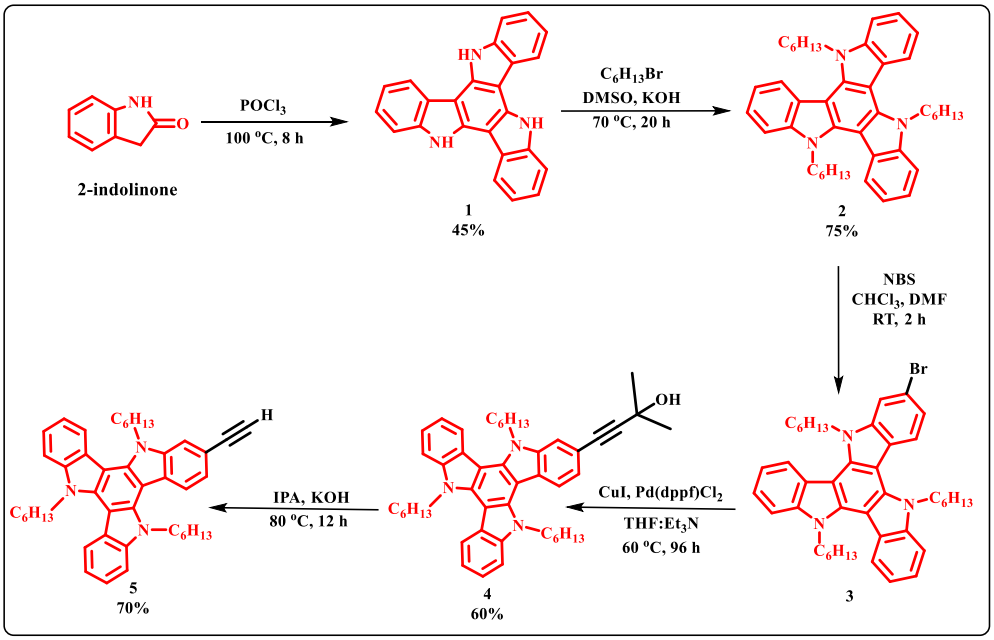
The design of Near–infrared (NIR) absorbing push–pull chromophores using the catalyst free [2+2] cycloaddition–retro electrocyclization (CA–RE) strategy by reacting an electron rich alkyne and strong acceptors (TCNE and TCNQ) have been used in the recent years for tuning optoelectronic properties of materials. The reaction of alkyne with tetracyanoethylene (TCNE) and TCNQ generates tetracyanobutadiene (TCBD) and Dicyanoquinodimethane (DCNQ) units respectively in the D–A systems.[24] . Expanded TCBD (also known as tetracyanohexatriene) and DCNQ units can be introduced using the terminal alkyne in place of internal alkyne.[7] This extended π–conjugation improves the donor–acceptor interactions, leading to lowered energy band gap, tailored thermal

and electrochemical properties. Different donor and acceptor counterparts such as triphenylamine, naphthalene–diimide (NDI)[25], carbazole, phenothiazine[26], truxene, diketopyrrolopyrrole (DPP)[27], isoindigo[13], azulene[28] have been incorporated with the TCBD unit to tune its properties. However, structural modification to modulate acceptor strength of expanded DCNQ frameworks is relatively underexplored.

In this work, D–A type push–pull chromophores, TAT1 and TAT2, were synthesized using triazatruxene (TAT) as the electron-donating unit and TCBD and DCNQ moieties as strong electron-accepting units in TAT1 and TAT2, respectively. The compounds were confirmed by thin layer chromatography and purified by column chromatography respectively. The compounds were analyzed by mass spectrometry, ^{1}H NMR, and ^{13}C NMR spectroscopic techniques. The main goal of this design strategy was to improve optical properties and to effectively tune the HOMO–LUMO energy gap, which is a key factor in determining electronic behavior. To understand their performance, we carried out detailed photophysical (light absorption and emission), electrochemical (redox behavior), and computational studies.

1.1 Aim and Strategy of our work

The aim of our work is to synthesize and characterize the derivatives of triazatruxene (TAT) core followed by evaluation of their photophysical, thermal and redox properties. Our objective is to investigate how modification to the TAT core affect charge transfer, HOMO–LUMO band gap, and thermal stability. By systematically analyzing these parameters, this study aims to contribute to the ongoing development of TAT–based donor–acceptor molecules for optoelectronic applications.



Scheme 1. Synthetic pathway to intermediate **1-5.**

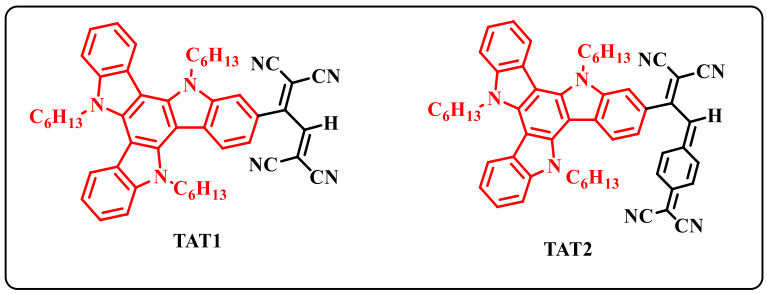
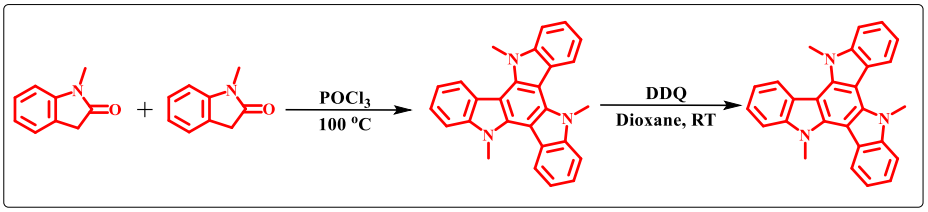


Figure 1.6. Chemical structures of **TAT1** and **TAT2.**

Chapter-2

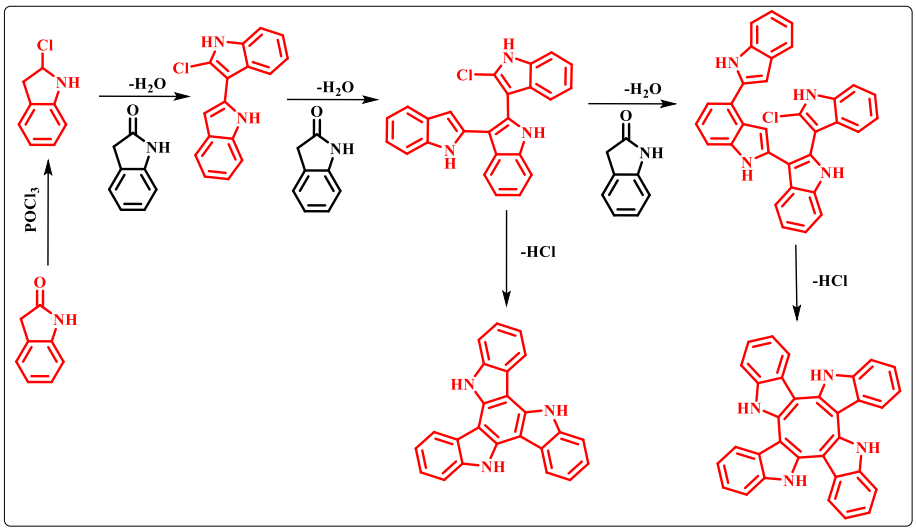
LITERATURE REVIEW

The earliest reported synthetic strategy to the triazatruxene framework was done in 1964. Muller synthesized N-trimethyltriazatruxene by heating 3-chloro-N-methylindole with aqueous sodium hydroxide in an autoclave at 180–200 °C in low yield.[29] Later, in 1980, Bergman and co-workers[30] observed that a symmetric cyclic indole trimer was formed as a side product in moderate yield during the copper-mediate oxidative coupling of indole for the synthesis of 2,2'-biindolyl derivatives. In the same period, the group also reported an alternative of 2-methylindole with 2-methyloxindole in the presence of $POCl_3$ at 100 °C, followed by cyclization induce by DDQ.



Scheme 2.1: Synthetic pathway by Bergman *et al*.

Nowadays, triazatruxene are commonly synthesized through a one-pot reaction starting from 2-oxindole, based on a modified method reported by Bergman and co-workers. The cyclotrimerization reaction in $POCl_3$ at 100 °C produces the unsubstituted triazatruxene as byproducts. Formation of the cyclic tetramer can be increased by dilution with chlorobenzene or excess $POCl_3$, although purification remain difficult due to the simultaneous formation of trimeric product.[31] Multistep formation of trimeric product and for tetraindole synthesis has also been reported. In addition, performing the reaction in an autoclave favours tetramer formation and simplifies purification of the final product.



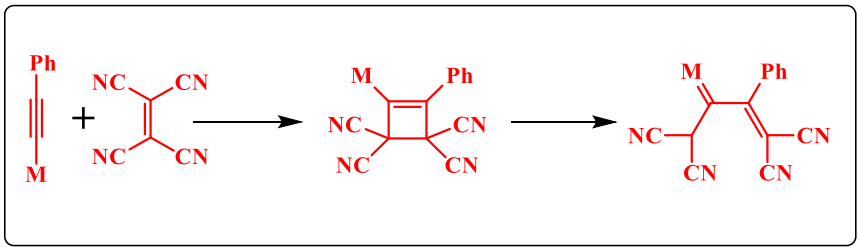
Scheme 2.2: Synthetic pathway of triazatruxene and tetraindole synthesis.

Different Synthetic methods for the preparation of TCNE analogues:

Three different synthetic methods of TCNE derivative have been reported (scheme 2.3–2.5).

Michael method:

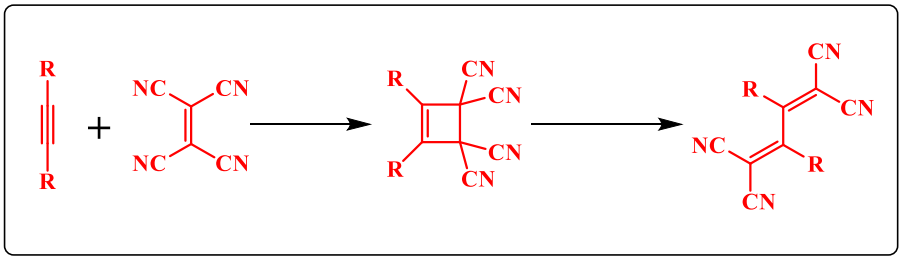
In 1981 work by Michael I. Bruce and co-workers[32] showed that electron-rich alkynes react with strong electron acceptors such as tetracyanoethylene (TCNE) under mild conditions. The reaction proceeds via a [2+2] cycloaddition to form a cyclobutene intermediate, which undergoes retroelectrocyclization to give 1,1,4,4-tetracyanobutadiene (TCBD) derivatives. The reaction typically provides good to high yields (≈70–90%) depending on the electron-donating strength of the alkyne substituents. These products act as strong electron acceptors and are widely used in donor–acceptor systems for optoelectronic applications.



Scheme 2.3. Michael method for TCNE derivative synthesis.

Yoshiro Yamashita method:

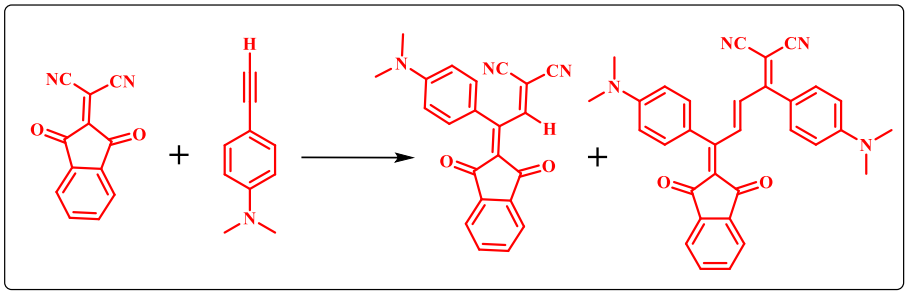
In 2004 Yamashita *et al*[33] reported the synthesis of donor–acceptor chromophores by reacting electron-rich acetylenes with tetracyanoethylene (TCNE). The reaction proceeds via a [2+2] cycloaddition followed by retroelectrocyclization, yielding tetracyanobutadiene (TCBD) derivatives. It is carried out under mild conditions (CH_2Cl_2, room temperature) and affords products in good yields (45–85%). The obtained compounds exhibit strong charge-transfer absorption and amphoteric redox behavior, making them suitable for optoelectronic applications.



Scheme 2.4. Yoshiro method for TCNE derivative synthesis.

Francois Diederich method:

Since 2015 François Diederich and co-workers[34] reported a simple and efficient method in which electron-rich alkynes react with TCNE or TCNQ via a [2+2] cycloaddition–retroelectrocyclization (CA–RE) reaction under mild, catalyst-free conditions. This reaction forms TCBD and DCNQ derivatives in good to excellent yields (≈60–95%), which exhibit strong charge-transfer properties and are useful in optoelectronic applications.



Scheme 2.5. Francois Diederich method for TCNE derivative synthesis.

Chapter-3

EXPERIMENTAL SECTION

3.1 General methods

All the chemicals that were used in the experiment were obtained unless indicated specifically. All the moisture responsive reactions were carried out in an argon environment. $CDCl_3$ was used as a solvent to record ^1H NMR (500 MHz) and ^{13}C NMR (125 MHz) spectra of both the compounds. The Chemical shifts are measured in parts per million (ppm) in reference to the solvent residual peak ($CDCl_3$, 7.26 ppm). In addition, s (singlet), d (doublet), and m (multiplet) are given in terms of Hz and coupling constants J. The chemical shifts in ^{13}C NMR are measured in reference to the solvent residual peak ($CDCl_3$, 77.16 ppm). The HRMS data were investigated using an ESI/APCI-TOF mass spectrometer. Dichloromethane (DCM) solvent was used to measure the spectra UV-visible absorption spectra of all the derivatives synthesized.

3.2 Experimental Procedure

3.2.1 Synthesis and characterization of compound 1:

A mixture of 2–indolinone (3 g, 0.0018 mol) and $POCl_3$ (15 mL) was taken in 50 mL RB, and heated at 100° C for 8h. Then, the reaction mixture was poured into ice and neutralized carefully with KOH. After neutralizing, the mixture was filtered to give the crude product as a brown solid. The crude residue was absorbed on silica– gel, dried, loaded and eluted through a thick silica–gel pad with DCM as mobile phase. After evaporation of solvent at reduced pressure and recrystallization from acetone, pure pale–yellow solid was obtained with 45 %. ^1H NMR (500 MHz, DMSO–d_6) δ = 11.87 (s, 3 H), 8.68 (d, J = 7.6 Hz, 3 H), 7.73 (d, J = 7.8 Hz, 3 H), 7.42 – 7.38 (m, 3 H), 7.36 – 7.32 (m, 3 H) ; ^{13}C NMR (125 MHz, DMSO–d_6) δ = 139.0, 134.3, 122.9, 122.7, 120.3, 119.6, 111.4, 101.0 ; HRMS (ESI–TOF) m/z calculated for $C_{24}H_{15}N_3$+H 345.1260 [M + H]+, measured

345.1217 [M + H]+.

3.2.2 Synthesis and characterization compound 2:

In a 100 mL RB, compound 1 (3 g, 0.00868 mol), KOH (5.8g ,0.104) and DMSO 25 ml were added. The reaction mixture was stirred at 70 °C for 1h. After 1h, 1–bromohexane (7.3 ml) was added to the reaction mixture and was refluxed for 19h. When the reaction was finished (TLC monitoring), the reaction mixture was cooled to room temperature and the mixture was extracted using ethyl acetate. The organic layer was dried over anhydrous Na_2SO_4. The residue mixture was purified by column chromatography using silica–gel and DCM and hexane to get the compound as white powder in 75% yield. ^{1}H NMR (500 MHz, CHLOROFORM–*d*) δ = 8.29 (d, J = 7.9 Hz, 3 H), 7.63 (d, J = 8.1 Hz, 3H), 7.45 (t, J = 7.6 Hz, 3 H), 7.37 – 7.31 (m, 3 H), 4.99 – 4.83 (m, 6 H), 2.05 – 1.88 (m, 6 H), 1.33 –1.18 (m, 19 H), 0.85 – 0.75 (m, 9 H); ^{13}C NMR (125 MHz, CHLOROFORM–*d*) δ =141.1, 138.9, 123.5, 122.7, 121.5, 119.6, 110.5, 103.2, 47.1, 31.4, 29.8, 26.4, 22.5, 13.9; HRMS (ESI –TOF) m/z calculated for $C_{42}H_{51}N_3$+H 597.4083 [M + H]+, measured 597.4094 [M + H]+.

3.2.3 Synthesis of compound 3:

In a 250 mL RB, compound 2 (1.9 g, 0.003180 mol) is taken in chloroform and NBS is dissolved in DMF. The solution of NBS is added dropwise in the RB at 0°C. The mixture was stirred for 1 h at RT. When the reaction was finished (TLC monitoring), compound was extracted using chloroform. The organic layer separated and passed through sodium sulphate. The crude mixture was loaded with silica and eluted using pure hexane to get the mixture as white powder. This mixture was further used for next reaction.

3.2.4 Synthesis and characterization compound 4:

In a 250 mL RB, compound 3 (3.2 g, 0.004738 mol) is taken and dissolved in THF:Et_3N (1:1) solvent and the mixture was degassed for 5 min. After degassing, the CuI (162 mg, 0.00085 mol) and Pd(dppf)Cl_2 (232 mg, 0.0002843 mol) was added followed by addition of 2-

methylbut-3-yn-2-ol (1 mL). The reaction mixture was stirred at 60°C for 96h. When the reaction was finished (TLC monitoring), the reaction mixture was cooled to room temperature. The residue was extracted using water and DCM. The organic layer separated and passed through sodium sulphate. The crude mixture was loaded with silica–gel and pure compound was eluted using DCM and hexane to get the compound as light–yellow powder in with 60% yield. ^{1}H NMR (500 MHz, CHLOROFORM–*d*) δ = 0.75 – 0.87 (m, 9 H) 1.20 – 1.34 (m, 18 H) 1.69 – 1.76 (m, 6 H) 1.90 – 2.03 (m, 6 H) 2.13 (s, 1 H) 4.81 – 4.96 (m, 6 H) 7.34 (t, *J*=7.48 Hz, 2 H) 7.40 (dd, *J*=8.24, 1.22 Hz, 1 H) 7.45 (t, *J*=7.55 Hz, 2 H) 7.63 (dd, *J*=7.93, 3.81 Hz, 2 H) 7.67 – 7.69 (m, 1 H) 8.17 (d, *J*=8.39 Hz, 1 H) 8.27 (t, *J*=7.48 Hz, 2 H); ^{13}C NMR (125 MHz, CHLOROFORM–*d*) δ = 141.0, 140.5, 139.6, 139.2, 138.6, 123.5, 123.4, 122.8, 121.6, 121.5, 121.1, 119.8, 119.8, 116.2, 113.6, 110.6, 110.5, 103.4, 103.1, 93.0, 83.6, 65.9, 47.1, 31.7, 31.4, 29.8, 29.8, 26.4, 22.5, 13.9. HRMS (APCI–TOF) m/z calculated for $C_{47}H_{57}N_3O$+H 679.4501 [M + H]+, measured 679.4485 [M + H]+.

3.2.5 Synthesis and characterization compound 5:

In a 100 mL RB, compound 4 (1.4 g, 0.002060 mol), KOH (1.61 g, 0.02884 mol) and 80 ml propanol were added. The reaction mixture was stirred at 80°C for 4 h. When the reaction was finished (TLC monitoring), the reaction mixture was cooled to room temperature. In the mixture residue solvent evaporate by rota. The residue was extracted using hexane and water. The organic layer separated and passed through Na_2SO_4. The crude mixture was loaded with silica–gel and pure compound was eluted using DCM and hexane to get the compound as viscous yellow liquid with 70% yield. ^{1}H NMR (500 MHz, CHLOROFORM–*d*) δ = 8.27 (t, *J* = 8.2 Hz, 2 H), 8.18 (d, *J* = 8.2 Hz, 1 H), 7.76 (s, 1 H), 7.66 – 7.60 (m, 2 H), 7.50 – 7.43 (m, 3 H), 7.35 (t, *J* = 7.6 Hz, 2 H), 4.94 – 4.82 (m, 6 H), 3.20 (s, 1 H), 2.02 – 1.92 (m, 6 H), 1.30 – 1.21 (m, 18 H), 0.82 (dt, *J* = 2.8, 7.0 Hz, 9 H); ^{13}C NMR (125 MHz , CHLOROFORM–*d*) δ = 141.0, 140.4, 139.7, 139.3, 138.6, 126.6, 125.7, 123.9, 123.7, 123.4, 123.3, 122.9, 121.6,

121.5, 121.2, 119.8, 119.8, 115.5, 114.2, 110.6, 110.6, 110.3, 103.4, 103.1, 85.3, 77.3, 77.0, 76.8, 76.3, 47.1, 31.4, 29.9, 29.8, 29.8, 26.4, 26.4, 26.3, 22.5, 13.9; HRMS (APCI–TOF) m/z calculated for $C_{44}H_{51}N_3$ +H 621.4083 [M + H]+, measured 621.4111 [M + H]+.

3.2.6 Synthesis and characterization of compound TAT1:

In a 100 mL RB, compound 5 (200 mg, 0.000161 mol) and TCNE (20mg, 0.00012059 mol) were dissolved in 20 mL DCM. The reaction mixture was stirred at RT for 2h. When the reaction was finished (TLC monitoring), the reaction mixture was evaporated by rota. The crude product was loaded with silica–gel and pure compound was eluted using DCM and hexane to get the compound as light green with 55% yield. ^{1}H NMR (500 MHz, CHLOROFORM–*d*) δ = 0.80 (s, 9 H) 1.22 (br. s., 18 H) 1.99 (br. s., 6 H) 4.73 – 4.87 (m, 2 H) 4.87 – 5.00 (m, 4 H) 7.22 (dd, *J*=8.47, 1.75 Hz, 1 H) 7.38 (t, *J*=7.40 Hz, 2 H) 7.50 (t, *J*=7.55 Hz, 2 H) 7.65 (d, *J*=8.09 Hz, 2 H) 7.89 (d, *J*=1.68 Hz, 1 H) 8.10 (s, 1 H) 8.21 – 8.30 (m, 3 H); ^{13}C NMR (125 MHz, CHLOROFORM–*d*) δ = 161.2, 155.2, 141.9, 140.9, 140.9, 140.9, 140.4, 138.4, 128.6, 123.6, 123.5, 123.1, 123.0, 122.0, 121.8, 121.5, 120.9, 120.6, 120.4, 113.0, 112.2, 111.7, 111.1, 111.0, 111.0, 108.8, 104.1, 103.3, 103.0, 97.9, 84.9, 47.2, 47.2, 31.4, 31.3, 31.3, 30.2, 29.8, 29.6, 26.3, 26.3, 22.4, 22.4, 13.9, 0.0; HRMS (APCI–TOF) m/z calculated for $C_{50}H_{51}N_7$ +H 750.4284 [M + H]+, measured 750.4284 [M + H]+.

3.2.7 Synthesis and characterization of compound TAT2:

In a 100 mL RB, compound 5 (100 mg, 0.000868 mol) and TCNQ (8 mg, 0.0000434 mol) were dissolved in DCE. The reaction mixture was stirred at 60°C for 12h. When the reaction was finished (TLC monitoring), the reaction mixture was cooled to room temperature. After completion of reaction, the mixture dried on rota and then extracted using DCM and water. The organic layer separated and passed through sodium sulphate. The crude mixture was loaded with silica–gel and was eluted using DCM and hexane to get the pure compound as brown powder with 60% yield. ^{1}H NMR (500 MHz,

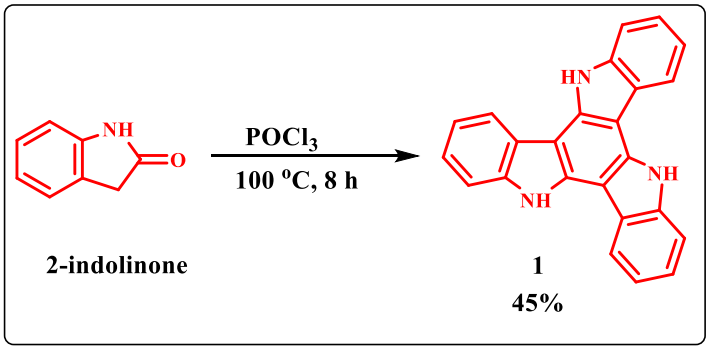
CHLOROFORM–*d*) δ = 0.73 – 0.84 (m, 10 H) 1.15 – 1.30 (m, 18 H) 1.88 (br. s., 2 H) 1.95 (br. s., 2 H) 2.01 (br. s., 2 H) 4.86 – 4.97 (m, 6 H) 7.01 (dd, *J*=8.24, 1.37 Hz, 2 H) 7.28 – 7.42 (m, 5 H) 7.51 (t, *J*=7.63 Hz, 2 H) 7.67 (dd, *J*=8.01, 4.81 Hz, 2 H) 8.07 (s, 1 H) 8.23 – 8.30 (m, 3 H); ^{13}C NMR (125 MHz, CHLOROFORM–*d*) δ = 154.1, 152.1, 146.4, 141.1, 141.0, 140.9, 140.8, 139.9, 138.6, 137.5, 128.0, 126.3, 123.6, 123.5, 123.2, 122.9, 121.9, 121.7, 121.6, 120.4, 114.2, 113.8, 111.1, 110.8, 110.2, 104.0, 103.4, 91.6, 79.2, 47.3, 47.3, 47.1, 31.9, 31.6, 31.4, 31.3, 29.9, 29.8, 29.7, 29.7, 29.6, 29.6, 29.4, 26.3, 26.2, 22.7, 22.4, 22.4, 22.4, 14.1, 13.9, 13.9, 0.0; HRMS (APCI–TOF) m/z calculated for $C_{56}H_{55}N_7$ +H 826.4597 [M + H]+, measured 826.4613 [M + H]+.

Chapter-4

RESULTS AND DISCUSSION

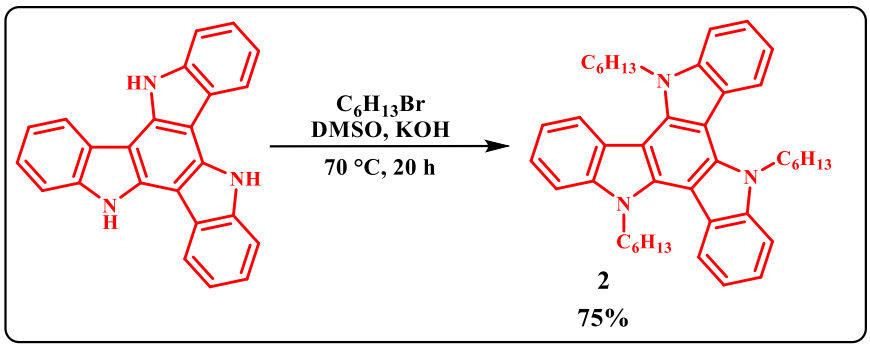
4.1 Synthetic pathway

Compound **1-5** was synthesized as shown in different schemes one by one. Compound **1** was synthesized *via* condensation of 2- indolinone in $POCl_3$ at 100 °C for 8h following the reported method. The compound **1** was obtained with 45% yield. (Scheme 3)



Scheme 4.1. Synthetic pathway of compound **1**.

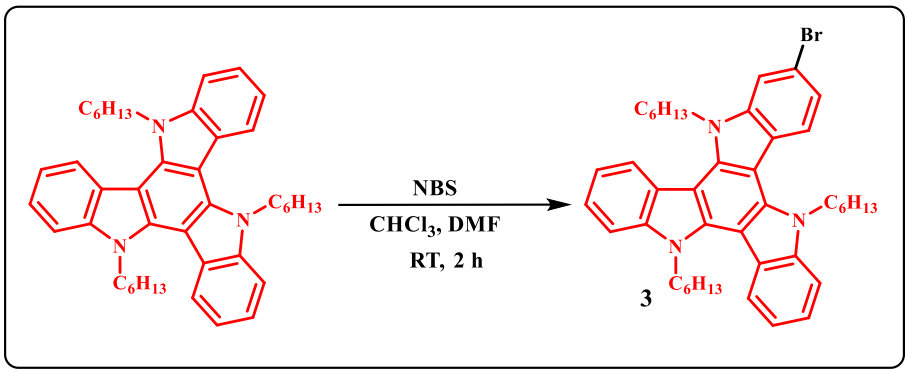
Compound **2** was synthesized by alkylating the free NH of compound **1** by treating with KOH followed with addition of 1-bromohexane in DMSO for 20 h at 70 °C following the reported method. The compound **2** was obtained with 75% yield. (Scheme 4)



Scheme 4.2. Synthetic pathway of compound **2**.

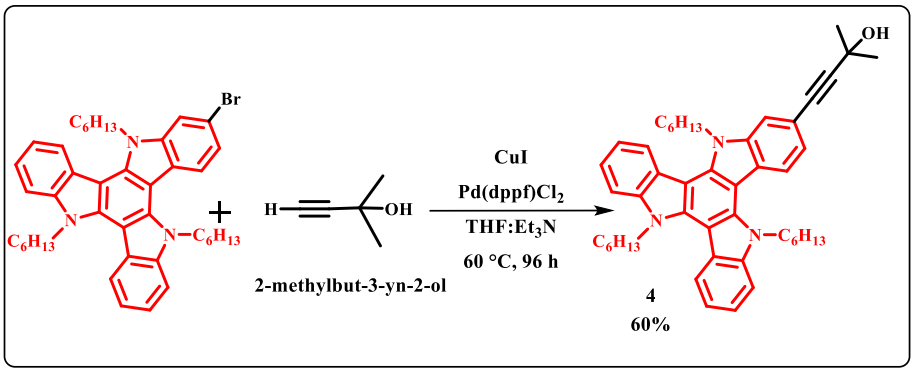
Compound **3** was synthesized by brominating compound **2** in chloroform by adding NBS in DMF dropwise at 0 °C following the

reported method. The compound **3** obtained used for further reaction without separation. (Scheme 5).



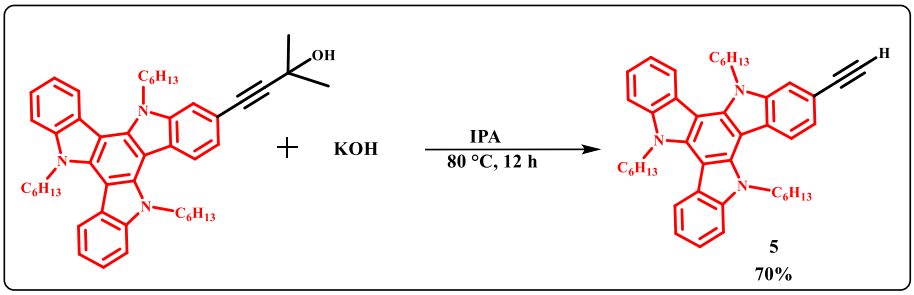
Scheme 4.3. Synthetic pathway of compound **3**.

Compound **4** was synthesized *via* sonogashira cross-coupling reaction treating the compound **3** with 2-methylbut-3-yn-2-ol in presence of CuI and $Pd(dppf)Cl_2$ catalyst, refluxing at 60°C for 96h in THF:Et_3N (1:1) solvent under inert atmosphere following the reported method. The compound **4** was obtained with 60% yield. (Scheme 6)



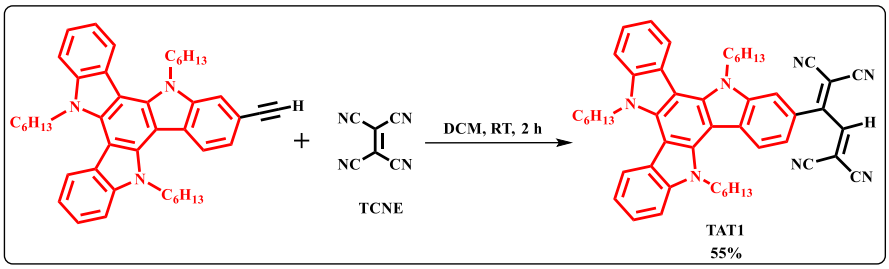
Scheme 4.4. Synthetic pathway of compound **4**.

Compound **5** was synthesized by deprotecting compound **4** by treating with KOH in IPA at 80 °C for 12 h with slight modification in the reported method. The compound **5** was obtained with 70% yield. (Scheme 7)



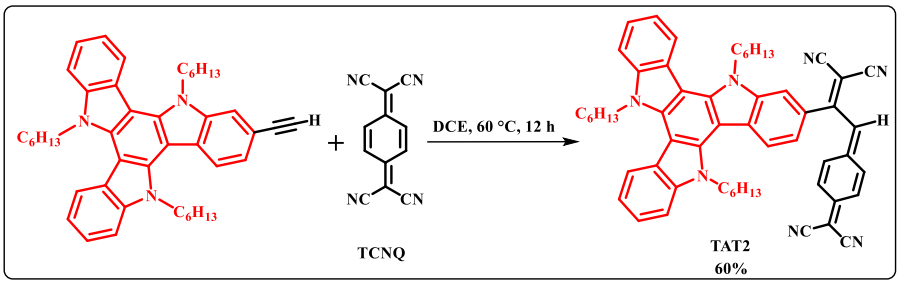
Scheme 4.5. Synthetic pathway of compound **5**.

Compound **TAT1** was synthesized using the catalyst free [2+2] cycloaddition–retro electrocyclization (CA–RE) reaction with tetracyanoethylene in dichloromethane at room temperature for 2 h. The compound **TAT1** was obtained with 55% yield. (Scheme 8)



Scheme 4.6. Synthetic pathway of compound **TAT1**.

Compound **TAT2** was synthesized using the catalyst free [2+2] cycloaddition–retro electrocyclization (CA–RE) reaction with 7,7,8,8-tetracyanoquinodimethane in dichloroethane at 60 °C for 12 h. The compound **TAT2** was obtained with 60% yield. (Scheme 9)



Scheme 4.7. Synthetic pathway of compound **TAT2**.

4.2. PHOTOPHYSICAL PROPERTIES

The electronic absorption spectra of D-A functionalized **TAT1** and **TAT2** were recorded at room temperature in DCM and is shown in Figure 2. The corresponding data is summarized in Table 1.

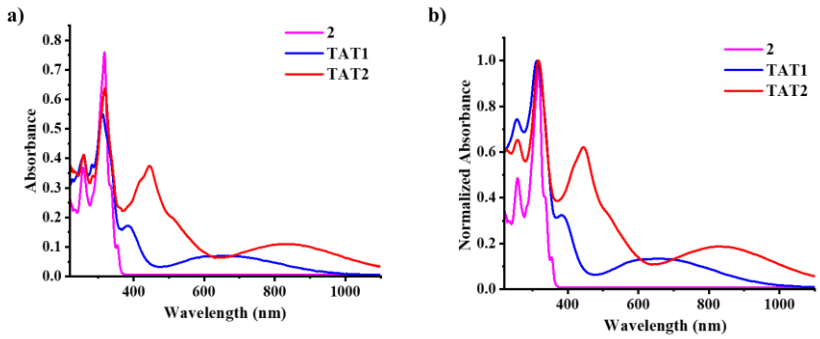


Figure 2. **a)** Unnormalized and **b)** normalized electronic absorption spectra of triazatruxene derivatives **TAT1** and **TAT2** recorded in DCM (1×10^{-5}M) at RT.

Triazatruxene absorbs in the range of 220-380 nm due to π to π* transition having two intense UV bands and second band with a shoulder around 353 nm. Apart from these three bands, one new absorption band was observed for **TAT1** and **TAT2** in NIR I region (650-850 nm) is attributed to charge transfer (CT) from triazatruxene donor to the acceptor TCBD and DCNQ counterparts. The third absorption band for compound **2** at 353 nm shifts to 383 nm and 445 nm in **TAT1** and **TAT2** respectively. A significantly larger bathochromic shift was observed for the third absorption band of **TAT2** (92 nm) relative to **TAT1** (30 nm) with respect to compound **2**, which can be assigned to the enhanced π-conjugation imparted by the incorporation of the DCNQ unit in **TAT2**. Moreover, both **TAT1** and **TAT2** shows higher molar extinction coefficients compared to compound **2**, as summarized in **Table 1**. Notably, the charge-transfer (CT) band of **TAT2** displayed a substantial bathochromic shift of 160 nm relative to **TAT1**, suggesting that the incorporation of the DCNQ unit is more efficient in extending absorption toward the lower energy NIR-I region than the TCBD unit.

Table 1. Photophysical and theoretical data of **TAT1** and **TAT2.**

Compound	λ_{abs} (nm)[a]	ε (M^{-1} cm^{-1})	E_g[a] (eV)	HOMO[b] (eV)	LUMO[b] (eV)	HOMO–LUMO[b] band gap
2	258	36890	2.7	–	–	–
	317	75660				
	353	10580				
TAT1	258	38731	0.85	−4.86	−1.06	3.80
	313	52195				
	383	16930				
	665	6963				
TAT2	258	38504	0.80	−4.80	−1.04	3.76
	317	58941				
	445	36584				
	825	10977				

[a]Absorption spectra were recorded in DCM (1×10^{-5} M conc). λ_{abs}: absorption maxima. ε: molar extinction coefficient. E_g[a]: Optical band gap. [b] HOMO, LUMO energy levels and energy band gap calculated from density functional theory.

4.3 ELECTROCHEMICAL PROPERTIES.

The cyclic voltammograms (CV) were recorded in order to determine the redox behaviour of compounds **TAT1** and **TAT2** and to evaluate the effects of acceptor substituents on the TAT using cyclic voltammetry. The measurements were conducted in dichloromethane with a 0.1 M solution of tetrabutylammonium hexafluorophosphate (Bu_4NPF_6), a glassy carbon electrode as a working electrode, an Ag/AgCl as a reference electrode, and a Pt wire as a counter electrode. The cyclic voltammograms of **TAT1, TAT2** and **2** are shown in Figure 3 respectively.

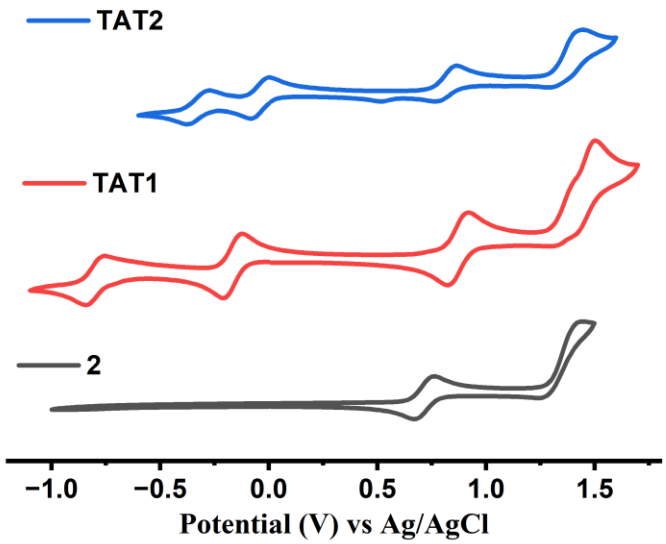


Figure 3. CVs of compound **TAT1, TAT2** and **2** in DCM at RT recorded in 0.1 M Bu_4NPF_6.

Compound **2** shows two oxidation waves at +0.76 and +1.44 V potential respectively. **TAT1** and **TAT2** exhibits two oxidation waves similar to the compound **2** but an anodic shift of oxidation waves was observed, indicating decrease in donor ability of triazatruxene on introduction of TCBD and DCNQ units. The two reduction waves appearing in the cathodic region for **TAT1** and **TAT2** belongs to TCBD and DCNQ units respectively. The first reduction wave was observed at -0.21 V and -0.08 V for **TAT1** and **TAT2** and second reduction wave was observed at -0.84 V and -0.38 V respectively. The lowered values of first oxidation and first reduction potentials observed for **TAT2** relative to **TAT1** indicate a comparatively narrower band gap in **TAT2**, which is consistent with the theoretically calculated band gap trend.

Table 2. Electrochemical data of **TAT1** and **TAT2.**

Compound	E^2 Oxid[a]	E^1 Oxid[a]	E^1 Red[a]	E^2 Red[a]
2	1.44	0.76	–	–
TAT1	1.51	0.92	-0.21	-0.84
TAT2	1.45	0.87	-0.08	-0.38

[a]Electrochemical analysis was carried out using a 0.1 M solution of Bu_4NPF_6 in DCM at a scan rate of 50 mVs^{-1} versus Ag/AgCl at 25 °C.

4.4 THEORETICAL CALCULATION

To understand the ground-state geometries and electronic structure of **TAT1** and **TAT2**, geometry optimizations were performed using density functional theory (DFT) theory level at B3LYP/6 311G+(d,p) level in the Gaussian 09W software. The frontier molecular orbitals are shown in figure 6. In both molecules, the HOMO is primarily localized over the triazatruxene core. In contrast, the LUMO in **TAT2** is mainly confined over the DCNQ unit, whereas in **TAT1**, the electron density is delocalized over the TCBD unit with substantial contribution from the triazatruxene core. The theoretical calculated values for HOMO have the same value (-5.70) for both the molecules, but the LUMO energy level is more stabilised in **TAT2** as compared to **TAT1** leading to lower band gap which is in good accord with the band gap trend calculated from the photophysical data.

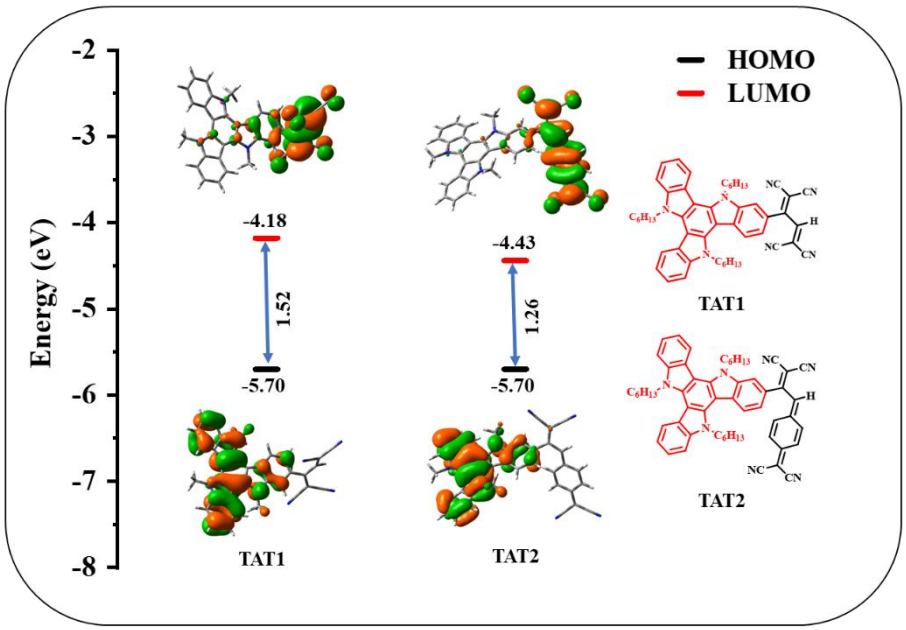


Figure 4. Frontier molecular orbitals of **TAT1** and **TAT2** calculated by DFT calculations at the B3LYP/6-311G + (d,p) level.

5. CONCLUSION

In summary, **TAT1** and **TAT2**, triazatruxene derivatives were designed and synthesized by using the catalyst free [2+2] cycloaddition–retro electrocyclization (CA–RE) reaction. The effects of acceptor TCBD and DCNQ units on photophysical and electrochemical properties of parent triazatruxene core were studied. The pronounced HOMO–LUMO charge redistribution suggests faster and efficient intramolecular charge-transfer (CT) processes with potential for charge separation prior to carrier recombination, rendering these derivatives promising for optoelectronic applications. Additionally, **TAT1** and **TAT2** shows broad absorption spanning the UV-Vis to NIR regions. Their intense panchromatic absorption across a wide spectral range, is likely to expand the horizons of triazatruxene-based derivatives for solar energy conversion and related photonic applications.

6. APPENDIX-A

1.1 ^{1}H NMR spectrum of Compound 1

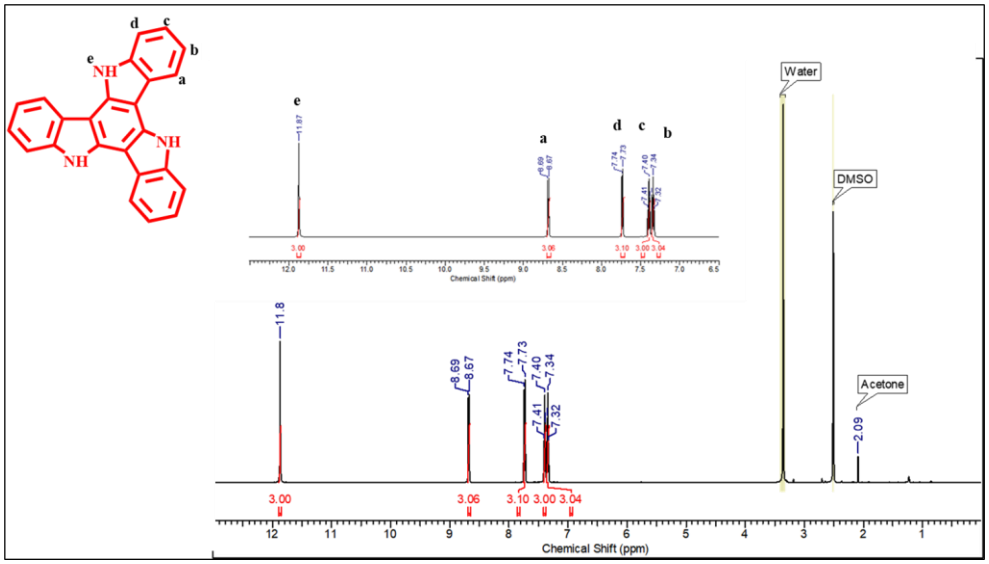


Fig. 5 ^{1}H NMR spectrum of compound **1**

1.2 ^{13}C NMR spectrum of Compound 1

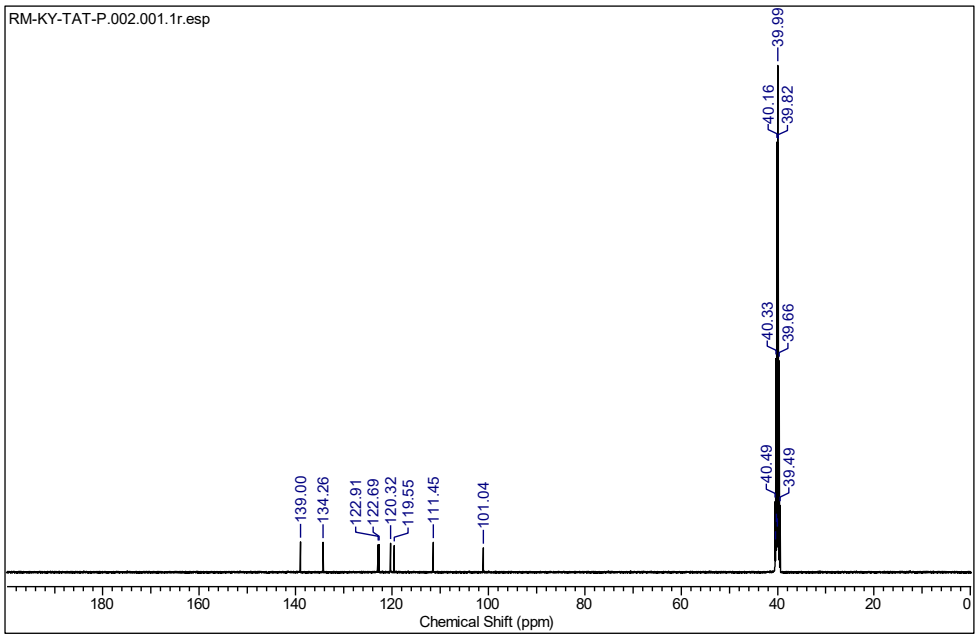


Fig. 6 ^{13}C NMR spectrum of compound **1**

1.2 Mass spectrum of Compound 1

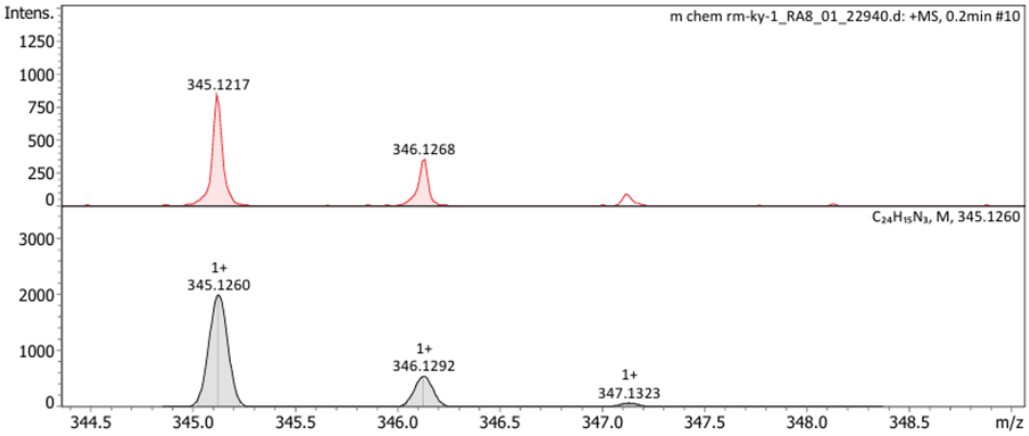


Fig. 7 HRMS of compound **1**

2.1 ^{1}H NMR spectrum of Compound 2

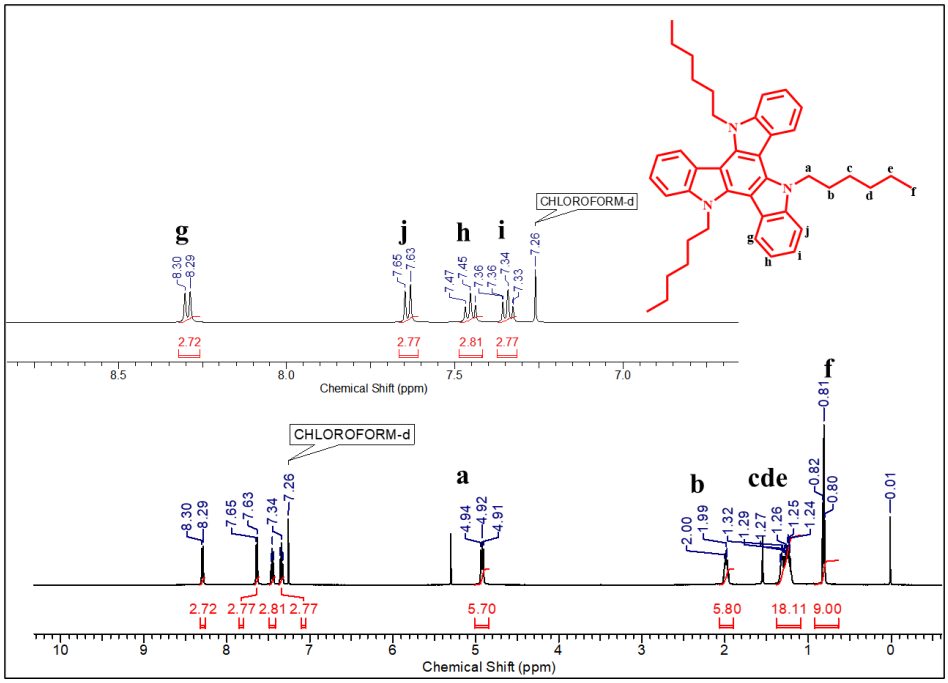


Fig. 8 ^{1}H NMR spectrum of compound **2**

2.2 ^{13}C NMR spectrum of Compound 2

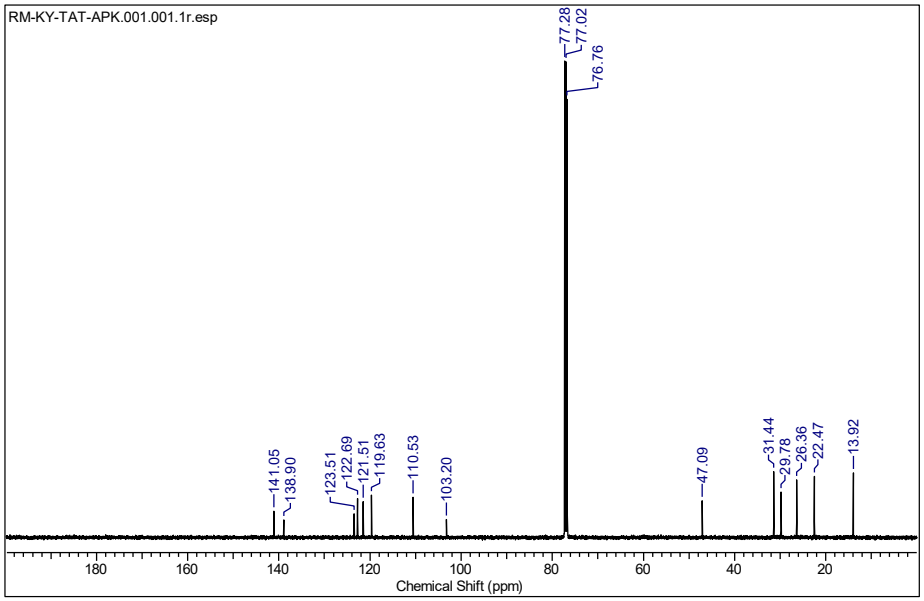


Fig. 9 ^{13}C spectrum of compound **2**

2.3 Mass spectrum of Compound 2

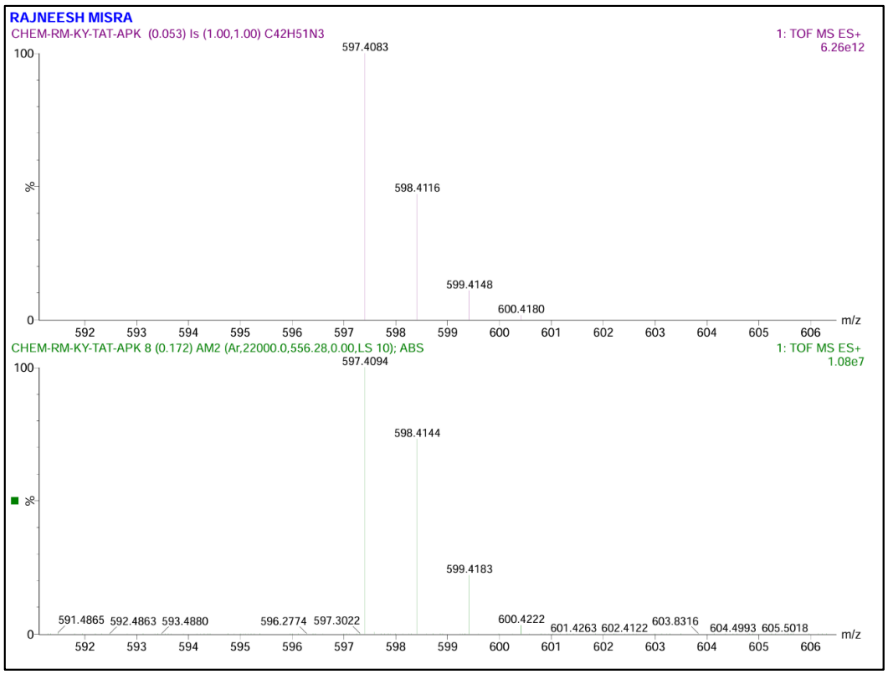


Fig. 10 Mass spectrum of compound **2**

4.1 ^{1}H NMR spectrum of Compound 4

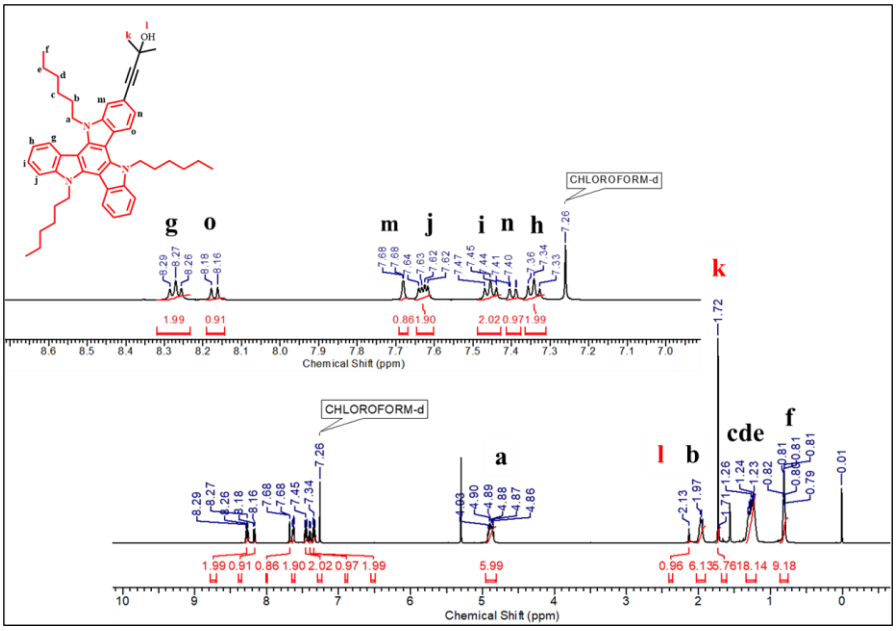


Fig. 11 ^{1}H NMR spectrum of compound **4**

4.2 ^{13}C NMR spectrum of Compound 4

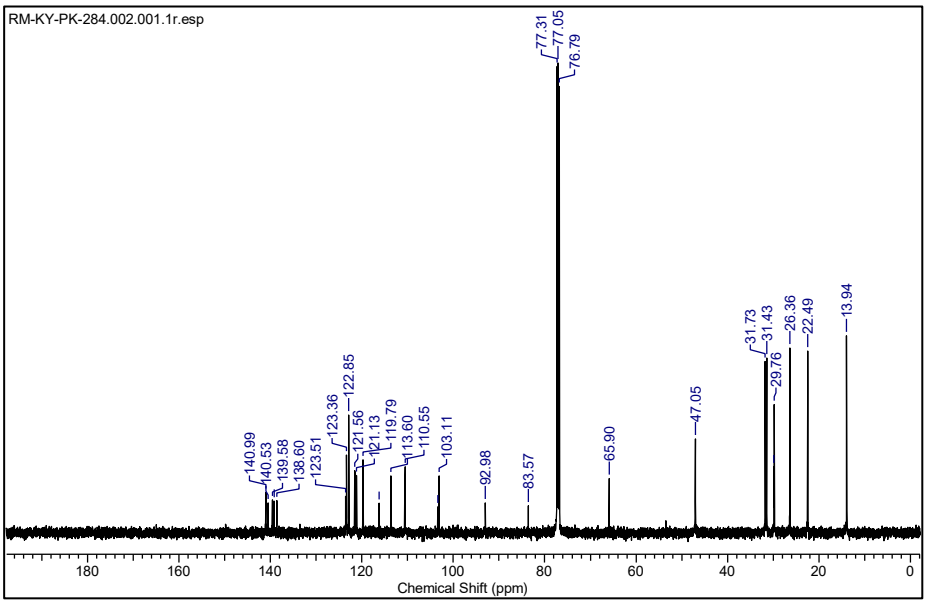


Fig. 12 ^{13}C spectrum of compound **4**

4.3 Mass spectrum of Compound 4

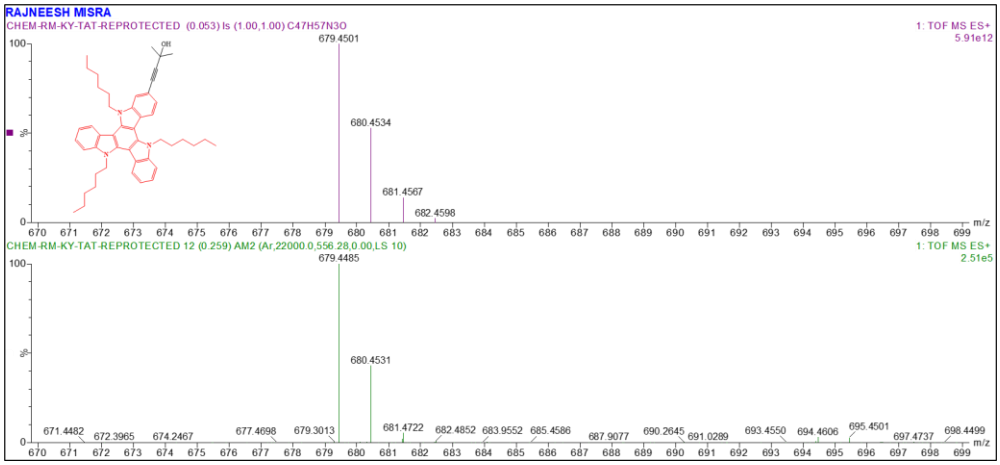


Fig. 13 HRMS of compound **4**

5.1 ^{1}H NMR spectrum of Compound 5

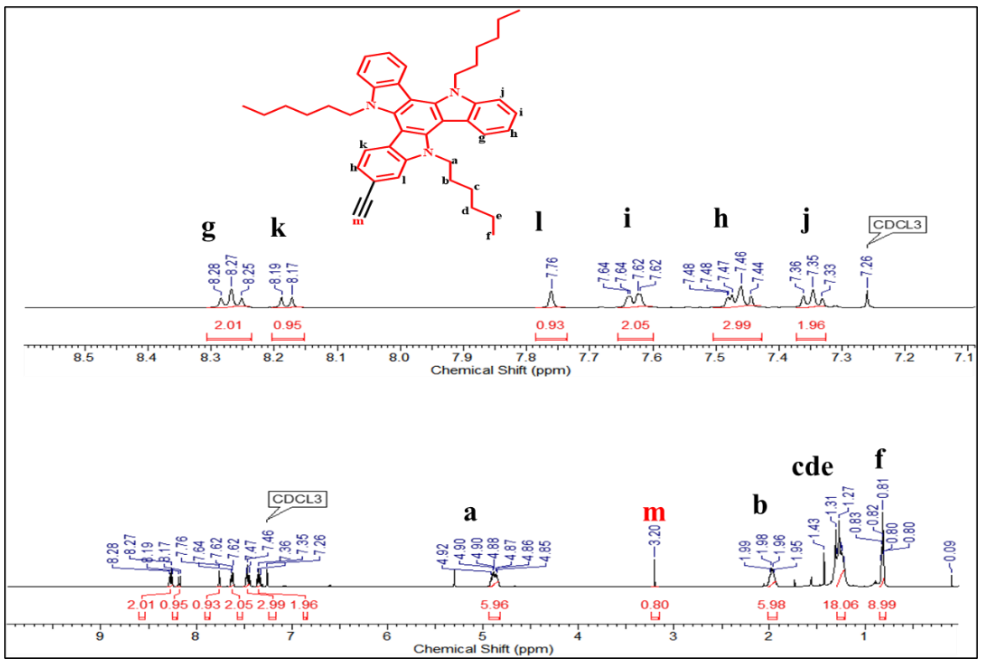


Fig. 14 ^{1}H NMR of compound **5**

5.1 ^{1}H NMR spectrum of Compound 5

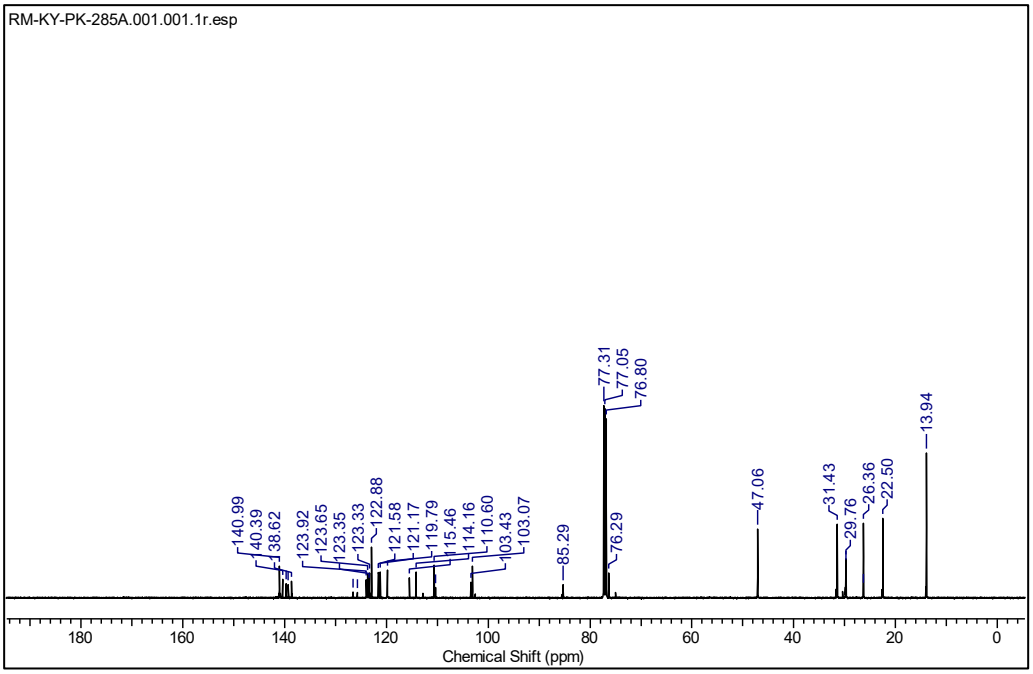


Fig. 15 ^{13}C spectrum of compound **5**

5.1 Mass spectrum of Compound 5

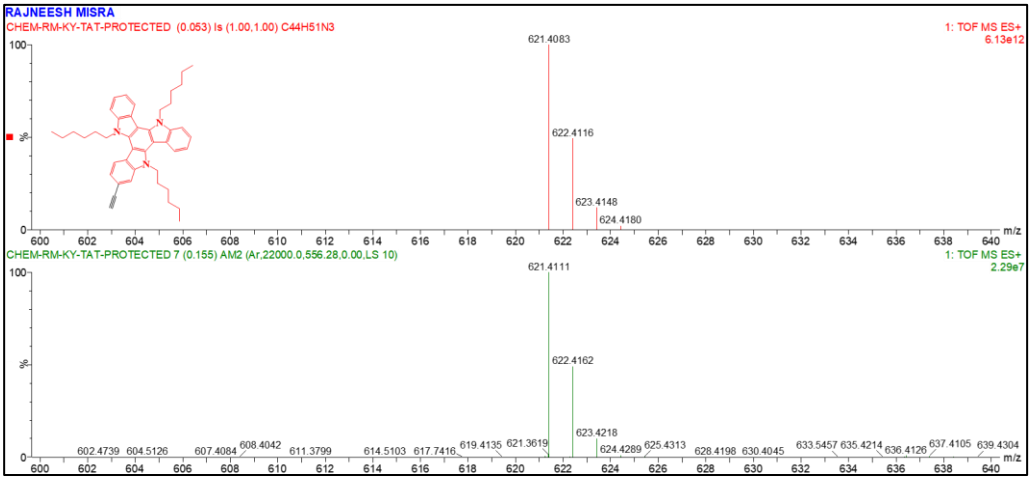


Fig. 16 mass spectrum compound **5**

6.1 ^{1}H NMR spectrum of Compound TAT1

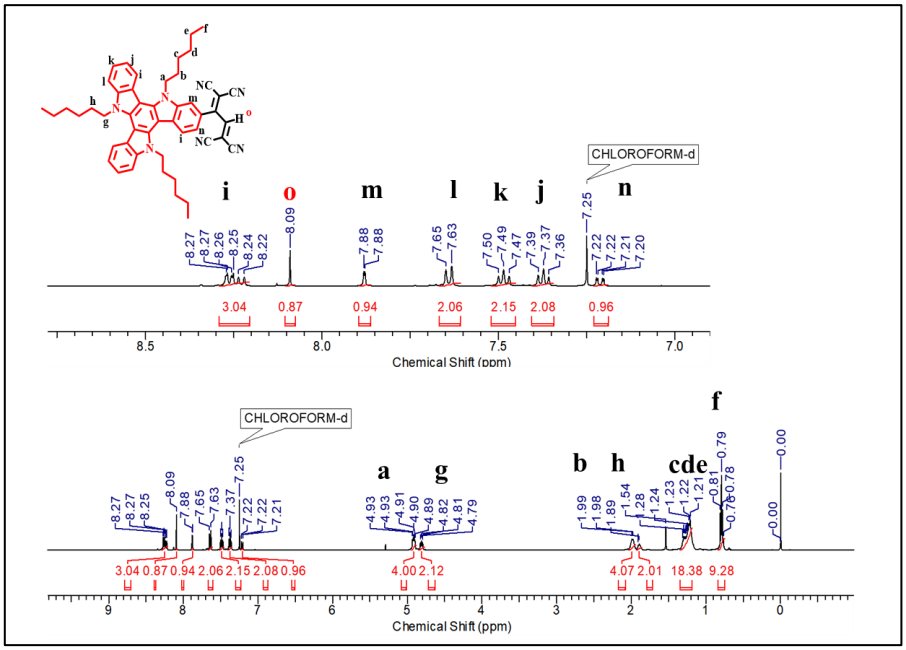


Fig. 17 ^{1}H NMR **TAT1**

6.2 ^{13}C NMR spectrum of Compound TAT1

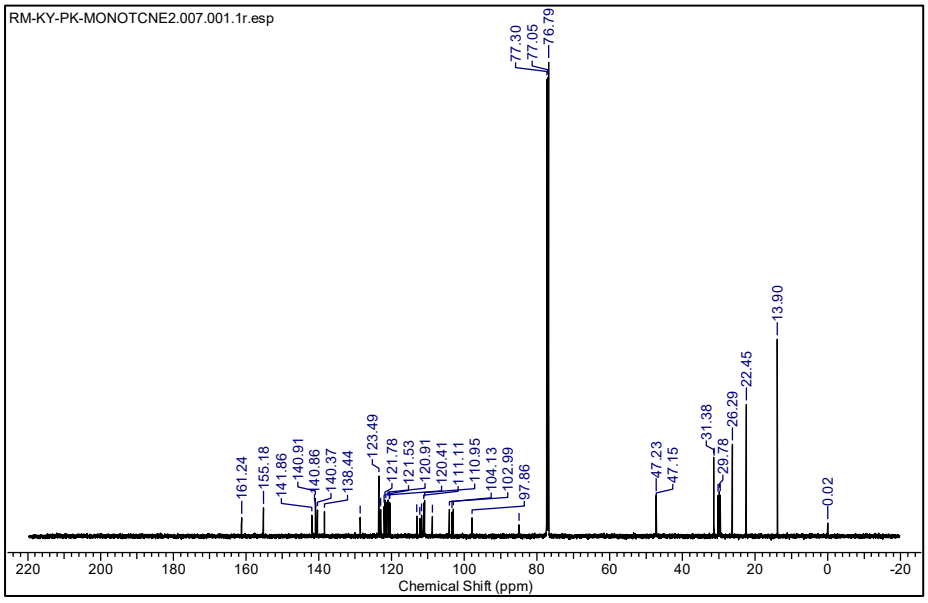


Fig. 18 ^{13}C spectrum of compound **TAT1**

6.3 Mass spectrum of Compound TAT1

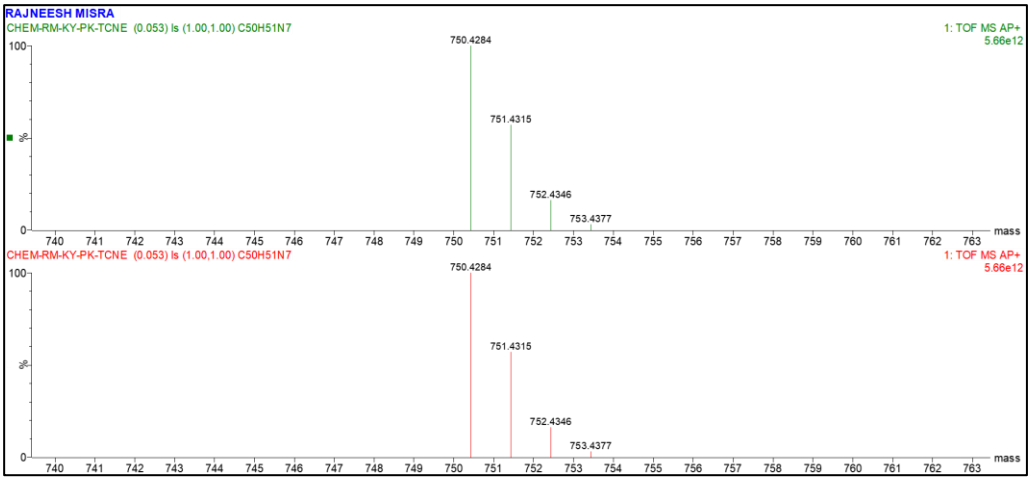


Fig. 19 mass spectrum of compound **TAT1**

7.1 ^{1}H NMR spectrum of Compound TAT2

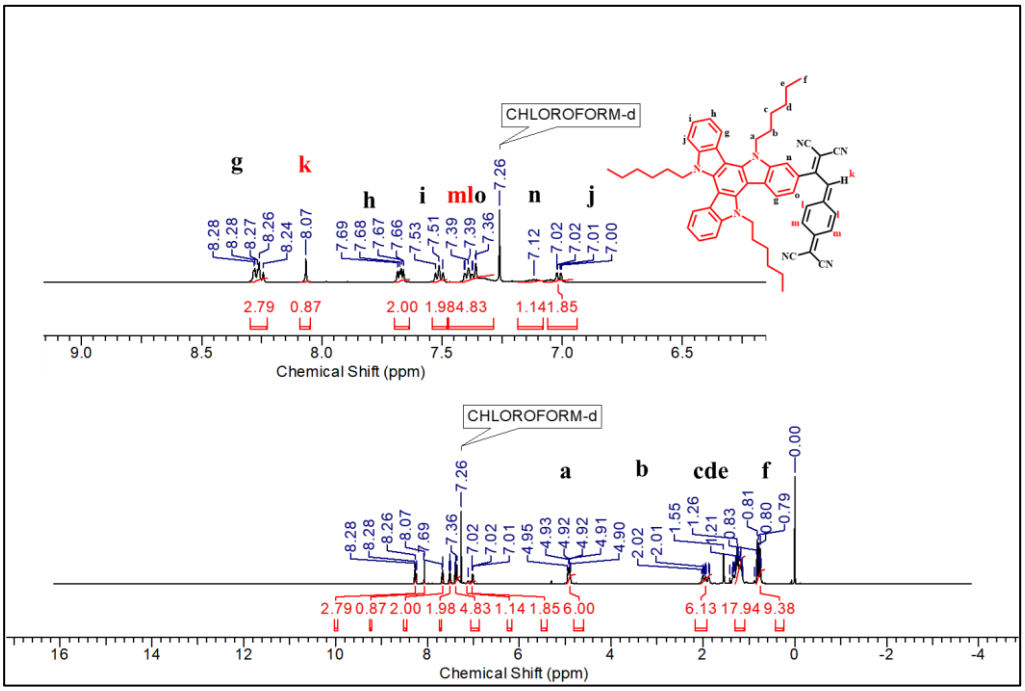


Fig. 20 ^{1}H NMR **TAT2**

7.2 ^{13}C NMR spectrum of Compound TAT2

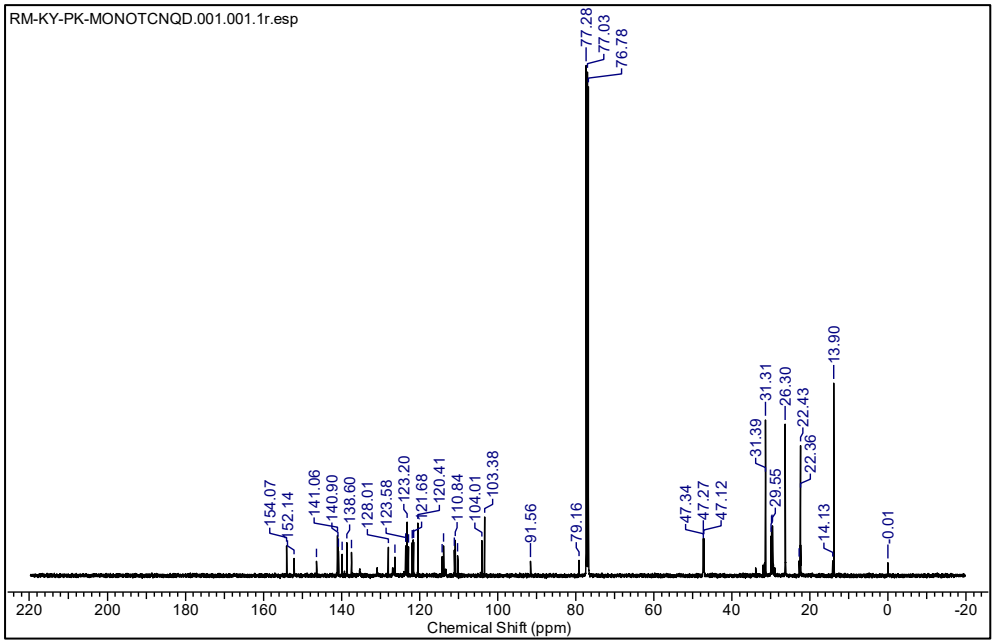


Fig. 21 ^{13}C spectrum of compound **TAT2**

7.3 Mass spectrum of Compound TAT2

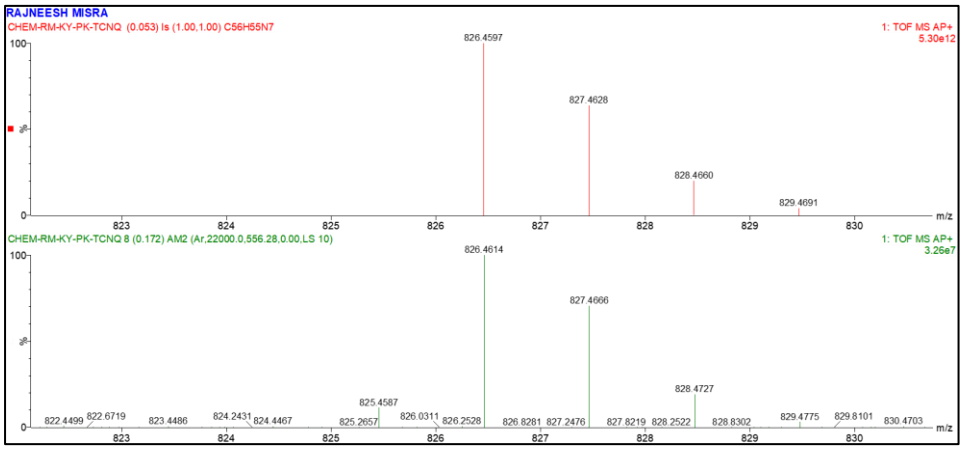


Fig. 22 mass spectrum of compound **TAT2**

REFERENCES

(1) Wazid, M.; Tarun; Pandey, U. K.; Misra, R. Donor-Functionalized Aza-Benzannulated Perylenediimide-Based Ternary Blend Efficient Inverted Organic Solar Cells. *J. Mater. Chem. C Mater.* **2025**, *13* (48), 24024–24035. https://doi.org/10.1039/d5tc03346b.

(2) Yang, X.; Xu, X.; Zhou, G. Recent Advances of the Emitters for High Performance Deep-Blue Organic Light-Emitting Diodes. *Journal of Materials Chemistry C*. Royal Society of Chemistry February 7, **2015**, pp 913–944. https://doi.org/10.1039/c4tc02474e.

(3) Babaei, A.; Rakstys, K.; Guelen, S.; Fallah Hamidabadi, V.; La-Placa, M. G.; Martínez-Sarti, L.; Sessolo, M.; Joel, H. A.; Gaudin, O. P. M.; Schanen, V.; Nazeeruddin, M. K.; Bolink, H. J. Solution Processed Organic Light-Emitting Diodes Using a Triazatruxene Crosslinkable Hole Transporting Material. *RSC Adv.* **2018**, *8* (62), 35719–35723. https://doi.org/10.1039/C8RA07184E.

(4) Huang, P.; Sheokand, M.; Payno Zarceño, D.; Kazim, S.; Lezama, L.; Nazeeruddin, M. K.; Misra, R.; Ahmad, S. Molecular Tailoring of Pyridine Core-Based Hole Selective Layer for Lead Free Double Perovskite Solar Cells Fabrication. *ACS Appl. Energy Mater.* **2023**, *6* (15), 7955–7964. https://doi.org/10.1021/acsaem.3c01027.

(5) Luizys, P.; Tian, S.; Rakstys, K.; Turnell-Ritson, R. C.; Paulauskas, V.; Jankauskas, V.; Getautis, V.; Nazeeruddin, M. K. Benzothiazole-Based Arylamines as Hole Transporting Materials for Perovskite Solar Cells. *J. Mater. Chem. C Mater.* **2025**, *13* (26), 13502–13508. https://doi.org/10.1039/d5tc01318f.

(6) Murai, M.; Tamaki, A.; Yamaguchi, S. Donor–Acceptor–Acceptor-Type Near-Infrared Fluorophores Featuring Thieno[3,2-b]Thiophene S,S-Dioxide and Diarylboryl Units as Dual Acceptors. *Org. Lett.* **2025**, *27* (34), 9436–9441. https://doi.org/10.1021/acs.orglett.5c02830.

(7) Kamble, A. V.; M, R. R. Electrochromic Properties of Tetracyanohexatriene Push-Pull Chromophores. *Chem. Asian J.* **2026**, *21* (2), e00902. https://doi.org/10.1002/asia.202500902.

(8) Nad, S.; Malik, S. Design, Synthesis, and Electrochromic Behaviors of Donor-Acceptor-Donor Type Triphenylamine-Iso-Naphthalenediimide Derivatives. *ChemElectroChem* **2020**, *7* (19), 4144–4152. https://doi.org/10.1002/celc.202001114.

(9) Cui, L.; Mei, S.; Yao, C. J. Donor-Acceptor Organic Electrode Materials: Regulating Molecular Orbital Energy Levels Toward Efficient Dual-Ion Storage. *Chemistry - A European Journal*. John Wiley and Sons Inc January 16, **2025**. https://doi.org/10.1002/chem.202503325.

(10) Neto, B. A. D.; Carvalho, P. H. P. R.; Correa, J. R. Benzothiadiazole Derivatives as Fluorescence Imaging Probes: Beyond Classical Scaffolds. *Acc. Chem. Res.* **2015**, *48* (6), 1560–1569. https://doi.org/10.1021/ar500468p.

(11) Koyyada, G.; Singh, S. P.; Bhanuprakash, K.; Han, L.; Bedja, I. M.; Gupta, R. K.; Islam, A.; Chandrasekharam, M. Study of Donor–Acceptor–π–Acceptor Architecture Sensitizers with Benzothiazole Acceptor for Dye-Sensitized Solar Cells. *Energy Technology* **2016**, *4* (3), 458–468. https://doi.org/10.1002/ente.201500431.

(12) Yashwantrao, G.; Saha, S. Recent Advances in the Synthesis and Reactivity of Quinoxaline. *Organic Chemistry Frontiers* **2021**, *8* (11), 2820–2862. https://doi.org/10.1039/D0QO01575J.

(13) Jiang, J.; Li, X.; Hanif, M.; Zhou, J.; Hu, D.; Su, S.; Xie, Z.; Gao, Y.; Yang, B.; Ma, Y. Pyridal[2,1,3]Thiadiazole as Strong Electron-Withdrawing and Less Sterically-Hindered Acceptor for Highly Efficient Donor–Acceptor Type NIR Materials. *J. Mater. Chem. C Mater.* **2017**, *5* (42), 11053–11058. https://doi.org/10.1039/C7TC03978F.

(14) Li, K.-C.; Huang, J.-H.; Hsu, Y.-C.; Huang, P.-J.; Chu, C.-W.; Lin, J.-T.; Wei, K.-H.; Lin, H.-C. Tunable Novel Cyclopentadithiophene-Based Copolymers Containing Various Numbers of Bithiazole and Thienyl Units for Organic Photovoltaic Cell Applications. *Macromolecules* **2009**, *42* (11), 3681–3693. https://doi.org/10.1021/ma900416d.

(15) Ahmed, E.; Subramaniyan, S.; Kim, F. S.; Xin, H.; Jenekhe, S. A. Benzobisthiazole-Based Donor–Acceptor Copolymer Semiconductors for Photovoltaic Cells and Highly Stable Field-Effect Transistors. *Macromolecules* **2011**, *44* (18), 7207–7219. https://doi.org/10.1021/ma201128x.

(16) Rout, Y.; Chauhan, V.; Misra, R. Synthesis and Characterization of Isoindigo-Based Push-Pull Chromophores. *Journal of Organic Chemistry* **2020**, *85* (7), 4611–4618. https://doi.org/10.1021/acs.joc.9b03267.

(17) Truong, M. A.; Funasaki, T.; Adachi, Y.; Hira, S.; Tan, T.; Akatsuka, A.; Yamada, T.; Iwasaki, Y.; Matsushige, Y.; Kaneko, R.; Asahara, C.; Nakamura, T.; Murdey, R.; Yoshida, H.;

Kanemitsu, Y.; Wakamiya, A. Molecular Design of Hole-Collecting Materials for Co-Deposition Processed Perovskite Solar Cells: A Tripodal Triazatruxene Derivative with Carboxylic Acid Groups. *J. Am. Chem. Soc.* **2025**, *147* (3), 2797–2808. https://doi.org/10.1021/jacs.4c15857.

(18) Chooppawa, T.; Namuangruk, S.; Yamamoto, H. M.; Promarak, V.; Rashatasakhon, P. Synthesis, Characterization, and Hole-Transporting Properties of Benzotriazatruxene Derivatives. *J. Mater. Chem. C Mater.* **2019**, *7* (47), 15035–15041. https://doi.org/10.1039/c9tc04155a.

(19) Górski, K.; Mech-Piskorz, J.; Pietraszkiewicz, M. From Truxenes to Heterotruxenes: Playing with Heteroatoms and the Symmetry of Molecules. *New Journal of Chemistry* **2022**, *46* (19), 8939–8966. https://doi.org/10.1039/D2NJ00816E.

(20) Aslan, M.; Taskesenligil, Y.; Plravadlll, S.; Saracoglu, N. Functionalization at Nonperipheral Positions of Triazatruxene: Modular Construction of 1,6,11-Triarylated-Triazatruxenes for Potentially Organic Electronics and Optoelectronics. *Journal of Organic Chemistry* **2022**, *87* (8), 5037–5050. https://doi.org/10.1021/acs.joc.1c02150.

(21) Vogelsang, L.; Birk, T.; Paschke, F.; Bauer, A.; Enenkel, V.; Holz, L. M.; Fonin, M.; Winter, R. F. Ferrocenyl-Substituted Triazatruxenes: Synthesis, Electronic Properties, and the Impact of Ferrocenyl Residues on Directional On-Surface Switching on Ag(111). *Inorg. Chem.* **2023**, *62* (39), 16236–16249. https://doi.org/10.1021/acs.inorgchem.3c03009.

(22) Chen, X.; Michinobu, T. Synthesis of Nonplanar Push–Pull Chromophores with Various Heterocyclic Moieties via [2 + 2] Cycloaddition-Retroelectrocyclization Reaction. *J. Org. Chem.* **2025**, *90* (4), 1561–1570. https://doi.org/10.1021/acs.joc.4c02595.

(23) Shoji, T.; Higashi, J.; Ito, S.; Okujima, T.; Yasunami, M.; Morita, N. Synthesis of Donor–Acceptor Chromophores by the [2 + 2] Cycloaddition of Arylethynyl-2H-Cyclohepta[b]Furan-2-Ones with 7,7,8,8-Tetracyanoquinodimethane. *Org. Biomol. Chem.* **2012**, *10* (12), 2431. https://doi.org/10.1039/c2ob06931h.

(24) Wang, D.; Guo, Q.; Gao, H.; Yang, Z.; Xing, Y.; Cao, H.; He, W.; Wang, H.; Gu, J.; Hu, H. The Application of Double Click to Synthesize a Third-Order Nonlinear Polymer Containing Donor–Acceptor Chromophores. *Polym. Chem.* **2016**, *7* (22), 3714–3721. https://doi.org/10.1039/C6PY00106H.

(25) Shoji, T.; Ito, S.; Toyota, K.; Iwamoto, T.; Yasunami, M.; Morita, N. Reactions between 1-Ethynylazulenes and 7,7,8,8-Tetracyanoquinodimethane (TCNQ): Preparation, Properties, and Redox Behavior of Novel Azulene-Substituted Redox-Active Chromophores. *European J. Org. Chem.* **2009**, *2009* (25), 4316–4324. https://doi.org/10.1002/ejoc.200900539.

(26) Das, S.; Rout, Y.; Poddar, M.; Alsaleh, A. Z.; Misra, R.; D'Souza, F. Novel Benzothiadiazole-based Donor-Acceptor Systems: Synthesis, Ultrafast Charge Transfer and Separation Dynamics. *Chemistry – A European Journal* **2024**, *30* (51). https://doi.org/10.1002/chem.202401959.

(27) Wazid, M.; Rout, Y.; Alsaleh, A. Z.; Kaswan, R. R.; Misra, R.; D'Souza, F. Perylenediimide Promoted Charge Transfer in Tetracyano Butadiene-Triphenylamine (TCBD-TPA) and Expanded-Tetracyano Butadiene-Triphenylamine (DCNQ-TPA) Push-Pull Conjugates. *Chemical Communications* **2025**, *61* (37), 6803–6806. https://doi.org/10.1039/d5cc00578g.

(28) Srinivasa Rao, P.; Brixi, S.; Shaikh, D. B.; Al Kobaisi, M.; Lessard, B. H.; Bhosale, S. V; Bhosale, S. V. The Effect of TCNE and TCNQ Acceptor Units on Triphenylamine-Naphthalenediimide Push-Pull Chromophore Properties. **2021**. https://doi.org/10.1002/ejoc.202100198[a.

(29) Gupta, P. K.; Khan, F.; Misra, R. NIR-Absorbing 1,1,4,4-Tetracyanobuta-1,3-Diene- and Dicyanoquinodimethane-Functionalized Donor-Acceptor Phenothiazine Derivatives: Synthesis and Characterization. *Journal of Organic Chemistry* **2023**, *88* (20), 14308–14322. https://doi.org/10.1021/acs.joc.3c01029.

(30) Patil, Y.; Butenschön, H.; Misra, R. Tetracyanobutadiene Bridged Push-Pull Chromophores: Development of New Generation Optoelectronic Materials. *Chemical Record*. John Wiley and Sons Inc January 1, **2023**. https://doi.org/10.1002/tcr.202200208.

(31) Shoji, T.; Ito, S. Azulene-Based Donor–Acceptor Systems: Synthesis, Optical, and Electrochemical Properties. *Chemistry - A European Journal* **2017**, *23* (66), 16696–16709. https://doi.org/10.1002/chem.201702806.

(32) Ruiz Domínguez, C. A. *New Organic Semiconductors Based on Triindole and Other Cyclic Oligomers of Indole ACKNOWLEDGMENTS*.

(33) Bergman, J.; Eklund, N. *SYNTHESIS OF 2,2'-BIINDOLYLS BY COUPLING REACTIONS*.

(34) Li, X.; Wang, C.; Xue, Y.; Meng, C.; Lai, W. Y.; Huang, W. Unexpected One-Pot Synthesis of Diindolotriazatruxene: A Planar Electron-Rich Scaffold Toward Highly π-Extended PAHs. *Asian J. Org. Chem.* **2017**, *6* (12), 1749–1754. https://doi.org/10.1002/ajoc.201700498.

(35) Bruce, M. I.; Rodgers, J. R.; Snow, M. R.; Swincer, A. G. Cyclopentadienyl-Ruthenium and -Osmium Chemistry. Cleavage of Tetracyanoethylene under Mild Conditions: X-Ray Crystal Structures of [Ru{η ^{3} -C(CN) $_{2}$ CPhC□C(CN) $_{2}$ }(PPh $_{3}$)(η-C $_{5}$ H $_{5}$)] and [Ru{C[□C(CN) $_{2}$]CPh□C(CN) $_{2}$ }-(CNBu ^{t})(PPh $_{3}$)(η-C $_{5}$ H $_{5}$)]. *J. Chem. Soc., Chem. Commun.* **1981**, No. 6, 271–272. https://doi.org/10.1039/C39810000271.

(36) Morioka, Y.; Yoshizawa, N.; Nishida, J.; Yamashita, Y. Novel Donor–π–Acceptor Compounds Containing 1,3-Dithiol-2-Ylidene and Tetracyanobutadiene Units. *Chem. Lett.* **2004**, *33* (9), 1190–1191. https://doi.org/10.1246/cl.2004.1190.

(37) Donckele, E. J.; Finke, A. D.; Ruhlmann, L.; Boudon, C.; Trapp, N.; Diederich, F. The [2 + 2] Cycloaddition–Retroelectrocyclization and [4 + 2] Hetero-Diels–Alder Reactions of 2-(Dicyanomethylene)Indan-1,3-Dione with Electron-Rich Alkynes: Influence of Lewis Acids on Reactivity. *Org. Lett.* **2015**, *17* (14), 3506–3509. https://doi.org/10.1021/acs.orglett.5b01598.